CHARACTERIZATION OF BIOMECHANICAL PROPERTIES OF THE BOVINE CORNEA IN TENSION

By
ABDOLRASOL RAHIMI

Bachelor of Science in Biomedical Engineering
Amirkabir University of Technology
Tehran, IRAN
2011

Submitted to the Faculty of the
Graduate College of the
Oklahoma State University
in partial fulfillment of
the requirements for
the Degree of
MASTER OF SCIENCE
July, 2014

CHARACTERIZATION OF BIOMECHANICAL

PROPERTIES OF THE BOVINE CORNEA IN TENSION

Thesis Approved:

Dr. Hamed Hatami-Marbini

Thesis Adviser

Dr. Don A. Lucca

Dr. Xiaoliang Jin

ACKNOWLEDGEMENTS

Foremost, I would like to thank Dr. Hamed Hatami–Marbini for his continuous advice, guidance and patience during my research work. He has been supportive since the first days I began working as a Master student. Besides my advisor, I would also like to thank the rest of my thesis committee: Dr. Don A. Lucca and Dr. Xiaoliang Jin. I do appreciate them for being my committee members and for their insightful comments. I thank Ebitimi Etebu, my labmate, for helping me in the experiments, continuously discussing about the research works, and his friendly advices.

I would like to express my sincere gratitude to my parents and sisters. They were always supporting me and encouraging me with their best wishes. I am grateful to all of friends and colleagues that helped and supported me in my research work and life. Acknowledgements reflect the views of the author and are not endorsed by committee members or Oklahoma State University.

Name: ABDOLRASOL RAHIMI

Date of Degree: July, 2014

Title of Study: CHARACTERIZATION OF BIOMECHANICAL PROPERTIES OF THE BOVINE CORNEA IN TENSION

Major Field: Mechanical Engineering

Cornea is a soft tissue with the principal function of transmitting and refracting light rays. It is composed of many different layers; epithelium, Bowman's layer, stroma, Decemet's membrane, and endothelium. It is well developed that biomechanical properties of the cornea are mainly due to the microstructure and composition of the stroma layer. The stroma constitutes 90% of the thickness and is mainly composed of collagen fibrils, proteoglycans, and interstitial fluid. The cornea in in-vivo condition is constantly subjected to membrane tensile stresses caused by the intraocular pressure. Therefore, a detailed understanding of its mechanical behavior in tension is required to enhance the accuracy of numerical models. Although uniaxial tensile experiments have been widely used to determine the tensile stress-strain behavior, available data in the literature shows a large variation.

In this thesis, a uniaxial tensile testing machine was first designed and built. This custom-made machine was used to investigate the effects of different parameters, such as loading rate, structural anisotropy, hydration, and riboflavin-UVA crosslinking, on immediate stress-strain and time dependent stress-relaxation behavior of the cornea. To this end, corneal strips with known dimensions were dissected from bovine eyes and were tested under immersed conditions. It was observed that the corneal stroma is a viscoelastic anisotropic material. In particular, the corneal strips obtained from the inferior-superior direction were significantly stiffer than those dissected from the nasal-temporal orientation. Moreover, the tensile stiffness of the samples increased with increasing the loading rate. Through testing corneal strips at different hydration levels, it was shown that hydration significantly affects the tensile properties; both tensile stiffness and stress significantly decreased with increasing hydration. Finally, the riboflavin and UVA irradiation were used to crosslink the corneas and investigate the biomechanical effects of collagen crosslinking treatment. It was seen that the riboflavin/UVA treated bovine corneal samples became significantly stiffer. The numerical exponential and power-law expressions were successfully represented the experimentally measured stress-strain curves. In conclusion, the present research study not only characterized the mechanical behavior of bovine cornea in tension, but it also provided new possible explanations for the existing wide variation in the reported corneal tensile behavior. The proper characterization of material properties is essential for developing more accurate computational models to predict corneal mechanical behavior.

Table of Contents

LIST OF TABLES

LIST OF FIGURES

SYMBOLS AND ABBREVIATION

IOP…….....Intraocular pressure

IS……Inferior-superior

NT……..Nasal-temporal

GAG …….…….Glycosaminoglycan

OBSS……..……Ophthalmic balanced salt solution

PBS……..…….Phosphate buffer solution

f……..……Frequency

δ……...Phase shift angle

E'……..……Storage modulus

E''……...…….Loss modulus

E^*……..……... Complex modulus

WAXRD……...……Wide angle x-ray diffraction

CXL…….....Crosslinking

LASIK……..……Laser In Situ Keratomileusis

Chapter 1

Introduction

1.1. Motivation

Cornea is a connective tissue with several important functions. It transmits visible light and focuses it on the retina. In order to function properly, the cornea needs to maintain its transparency and high mechanical stability. High amount of collagen fibers in the cornea gives the desired strength for bearing intraocular pressure and the possible impact from outside. Any disorder in the ultrastructure of cornea could affects its biomechanical properties.

For example, laser in situ keratomileusis (LASIK) is a common eye surgery with over 30 million operations being carried out every year[1]. In LASIK, a cut is made through the cornea to create a flap, Figure 1.1(left). The cut through the stroma will damage considerable percentage of collagen fibrils and could possibly result in Keratoconus[2], Figure 1.1(right). Keratoconus is an eye disorder in which the cornea becomes soften and the corneal curvature increases.

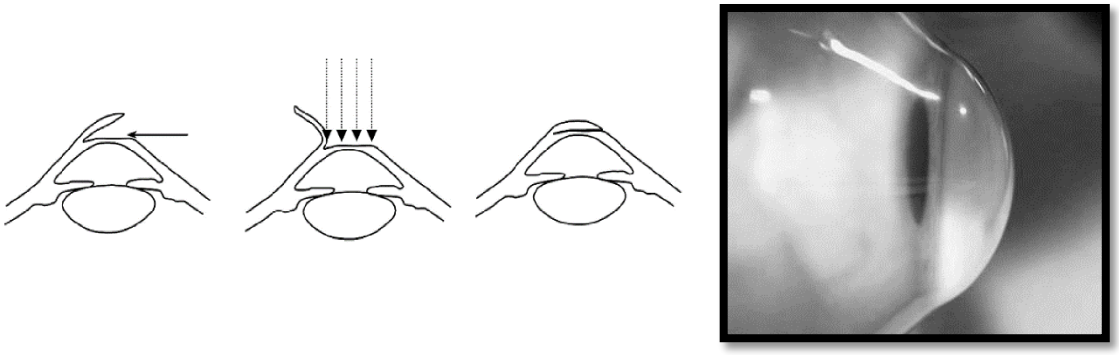

Figure 1.1. (Left) LASIK procedure. The cut through the stroma will damage considerable percentage of collagen fibrils (with permission from[1]), (Right) Keratoconus cornea (adapted from http://keratoconusinfo.files.wordpress.com/2009/12/right_lens1.jpg).

To find the new treatment or improve the current treatment methods, it is needed to have a comprehensive understanding about the mechanics of the cornea.

There are different ways to measure the mechanical properties of the cornea. One of the most commonly used method is the in vitro uniaxial tensile experiments. In this thesis, this testing method is used to determine the stress-strain, stress relaxation and dynamic mechanical properties of the cornea in tension. In addition, influence of collagen crosslinking treatment on the stiffness and corneal properties is investigated.

1.2. Specific aims

The specific aims of this thesis are:

1) Characterizing the rate dependent and anisotropic tensile behavior of bovine cornea

2) Determining possible effects of bathing solution on tensile behavior of bovine cornea

3) Characterizing hydration dependent tensile properties of bovine cornea

4) Investigating the stiffening effects of corneal collagen crosslinking on stress-strain behavior of the cornea in tension

1.3. Approach

An uniaxial tensile test was used to characterize biomechanical response of the cornea. Steady state, time dependent stress relaxation, and dynamic behavior of cornea were used to study mechanical properties of cornea. Different displacement rates were used to investigate strain rate dependency properties of cornea. In addition, anisotropy was examined by conducting tensile test on the NT and IS strips under same conditions. Bathing fluids including Saline solutions, DI-water, PBS, OBSS, and Mineral oil were used to fill the submersion chamber during uniaxial tensile test to analyze the effect of swelling on the mechanical behavior of cornea. Water content and thickness influence on the corneal stiffness was conducted by using mineral oil as a bathing fluid. Mineral oil maintained the hydration constant. Collagen crosslinking treatment effect on biomechanical properties of cornea was investigated using uniaxial tensile, stress relaxation, and frequency sweep tests.

Chapter 2

Background

2.1. Ultrastructure of cornea

Eye is the gate to see the outside world. Eyeball position, skull shape, and muscles around eyeball protect eye from injury[3]. In addition to impact injury, different diseases may affect visual ability and biomechanical properties of eye. Keratoconus, glaucoma, and cataract are some examples of eye disorders. There have been different studies for improving vision ability and finding treatments for patients[4-6].

Cornea is a barrier between outside world and inside of eye as shown in Figure 2.1. It is a connective tissue with several important functions. Cornea transmits visible light and focuses on the retina. In order to function properly, the cornea needs to maintain its transparency and high mechanical stability which ensures maintaining the shape and curvature of eye.

The central curvature is 7.8 mm which is larger in the nasal-temporal (NT) direction than inferior-superior (IS) direction. Human corneal diameter is about 11 mm and it is slightly bigger in the NT direction than IS direction[7]. The central human corneal thickness is 0.5 mm which increases in the periphery[1]. The anatomy of eye globe varies among

mammalians. Bovine corneal diameter, curvature, and thickness are 20 mm, 17.5 mm, and 0.75-0.87 mm[1], respectively.

Cornea is a highly organized tissue and constitutes of five layers, in Figure 2.2: epithelium, Bowman's layer, stroma, Decemet's membrane, and endothelium, respectively from anterior to superior side.

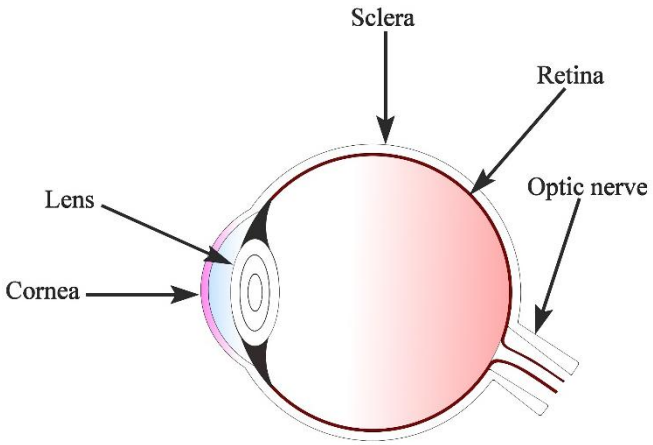

Figure 2.1. Main organs of eye.

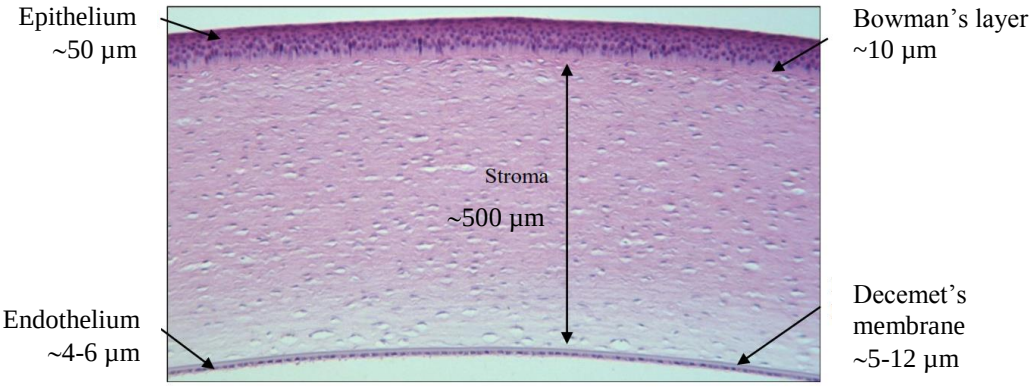

Figure 2.2. Stroma layers and their thicknesses of human cornea
(Adapted from http://www.vetmed.ucdavis.edu/courses/vet_eyes/images/archive/s_4015_a.jpg).

1. Epithelium: The epithelium is a stratified layer with 50 µm thickness. Eye blinking moisturizes the epithelium surface and keeps it smooth. Epithelium cells turnover every 7 days[8].

2. Bowman's membrane: Bowman's membrane is an acellular layer with 10 µm thickness composed of randomly organized collagen fibrils mainly types I, III, V, and VIII [9]. The fibrils inside the membrane form a network that functions as a connection between epithelium and stroma.

3. Stroma: The stroma forms 90% of the corneal thickness and is mainly responsible for the mechanical properties of cornea. Stroma is the stratified part of cornea with compact ultrastructure composed of collagen fibril rich extracellular matrix. Stroma comprises keratocytes, extracellular matrix, neural tissue, and fibroblastic cells[10]. Collagen fibrils are bundled in thin sheets called lamella. The lamella distribution is equal in the vertical and horizontal direction[11]. While in the posterior side of stroma, they cross each other orthogonally, in the anterior part, they are not well organized and interweave each other[9]. In each lamella, the collagen fibrils are aligned in a specific direction. In the human cornea, diameter of collagen fibrils is 31-34 nm in the center and increases to 50 nm in the periphery[12]. The interfibrillar distance has been measured using x-ray scattering. While Ehlers and Hjortdal[7] reported 40-45 nm, in the Fratzl's study[9], the interfibrillar distance is presented as 57 nm in the center and 62 nm at the limbus. Different types of collagen exist in the cornea with specific functions and distributions; Collagen type I (58%), collagen type V (15%), VI (24%), and small amount of XII and XIV are available, too[7, 9, 13]. It is

assumed that the collagen type XII controls the interfibrillar distance by forming the interfibrillar bridges.

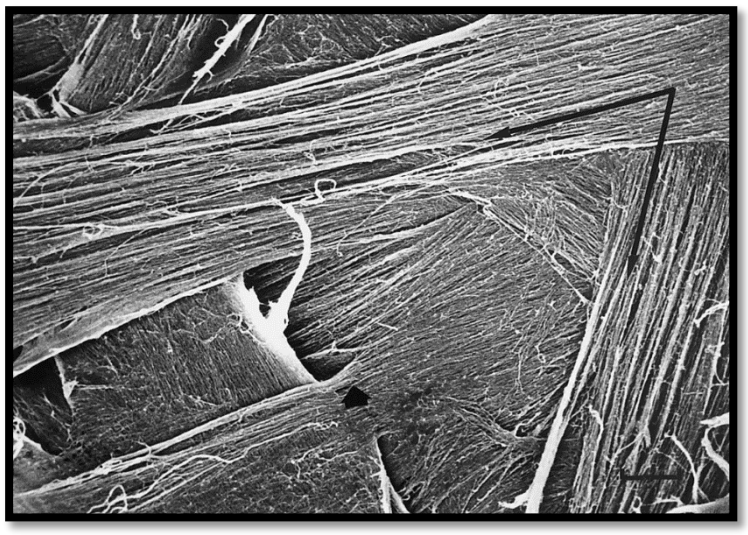

Figure 2.3. Collagen fibrils are bundled in thin sheets called lamella. In each lamella, the collagen fibrils are aligned in a specific direction (with permission from[14]).

Proteoglycans and other proteins exist in the extracellular matrix which fills interfibrillar spaces. Proteoglycans have a core protein molecule with covalent bonds to glycosaminoglycan (GAG) side chains. Proteoglycans connect to the surface of collagen fibrils[15]. Because GAGs have a negative charge and are hydrophilic, hydration of cornea highly depends on the proteoglycans density and distribution[9, 15]. Chondroitin sulphate, dermatan sulfate, heparan sulfate, and keratan sulfate are the four proteoglycans in the stroma.

Wide angle x-ray diffraction (WAXRD) is used in many of previous research to study distribution of fibers through the cornea. The obtained pattern showed that collagen fibrils are mainly oriented in the in radial direction and also fibril density is higher in the two orthogonal directions[16]. Daxer and Fratzel[11] reported fibril orientation is not uniform and

density of fibrils in the 45º sector around IS and NT direction is twice as oblique sections: therefore,, human cornea is stiffer in the IS and NT directions than oblique directions. This anticipation has been confirmed in the uniaxial tensile test[17]. A recent study by Meek and Boote[18] proposed a distribution pattern, based on the intensity of the x-ray images, that illustrates some lamellas crossing the cardinal points without entering the central zone.

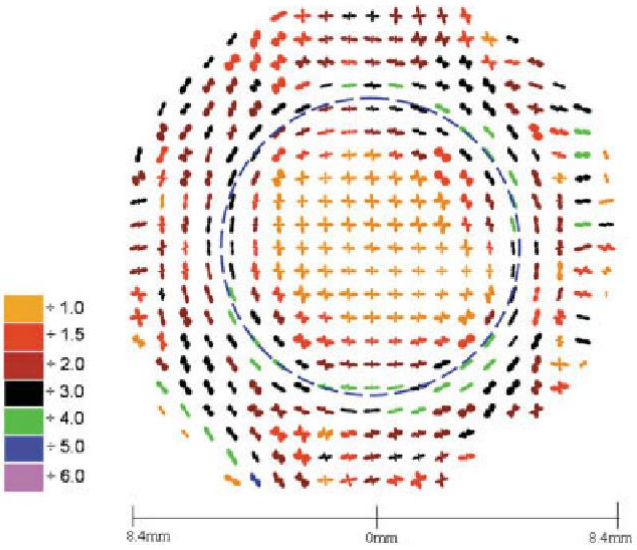

Figure 2.4. Vector plot maps obtained using WAXRD showing that there are collagen fibrils in all radial direction and also fibril density is higher in the two orthogonal directions for human cornea[16].

4. Descemet's membrane: Decemet's membrane is a thick basal lamina placed between stroma and endothelium. The layer thickness increases with the age from 5 to 12 µm[10].

5. Endothelium: Endothelium is a 4-6 µm single cell layer which contains about 400,000 cells. Endothelium does not change or regenerate in the whole life[10]. The most important function of endothelium is to keep the hydration of cornea in the physiological range[9].

2.2. Mechanics of cornea

Mechanics of cornea has been studied using several mechanical testing methods: inflation test, unconfined compression experiment, and uniaxial tensile test. Inflation test setup as shown in Figure 2.5, is used to simulate the physiological condition in the laboratory[19-21]. For the normal eyes, an initial intraocular pressure in the range of 1.4 to 2.8 KPa[1] is applied inside eye globe or on the posterior side of corneal scleral ring. Next, the pressure is raised and the apical rise is measured using the imaging techniques. The inflation test has following complications and limitations. Pressure change will cause deformation in not only cornea but also sclera and it is difficult to measure deformations separately; thus ascribing all of deformation to cornea produces error in the results. In addition, using fluid to manage the pressure results in corneal swelling which affects displacement and mechanical behavior of cornea.

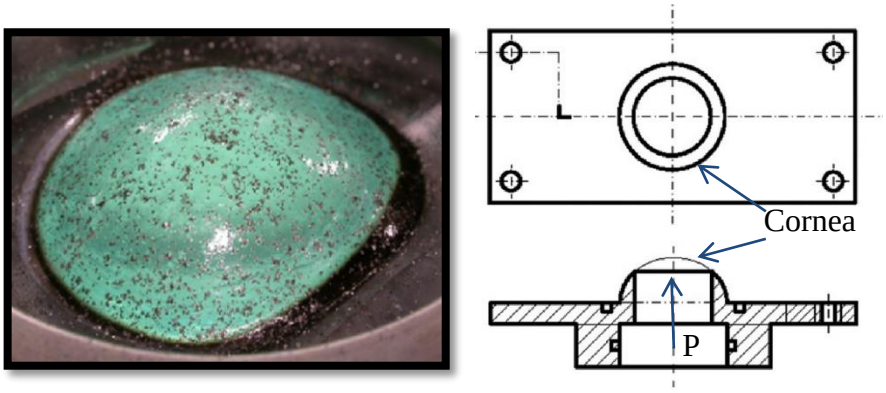

Figure 2.5. (Left) The bovine cornea in the inflation test with flakes on the surface, (Right) schematic plot of device set up for inflation test[22]. In the inflation test, an initial pressure in this range applies inside eye globe or on the posterior side of corneal scleral ring. Next, the pressure is raised and the apical rise is measured using the imaging techniques (with permission from[19]).

Compression test is a well-established experimental method to characterize mechanical behavior of tissues such as articular cartilage[23, 24]. In this experiment, the specimen is placed between a fixed platen and another platen that moves down and applies pressure as shown in Figure 2.6. There are two procedures for compression experiments, confined and unconfined compression. In the first method, the specimen is confined radially in a chamber, so there is no radial expansion and the above platen is permeable. In contrast, in the unconfined compression the specimen is free to expand in radial direction and two platens are impermeable.

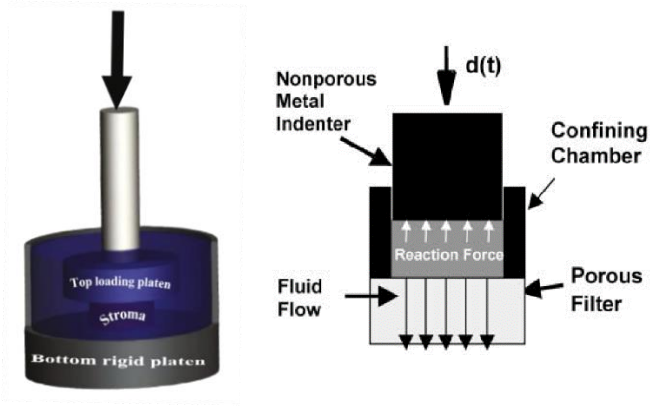

Figure 2.6. In the compression test, the specimen is placed between a fixed platen and another platen that moves and applies pressure. There are two procedures for compression experiments, unconfined (left) and unconfined (right) compression (with permission from [25, 26]).

The uniaxial tensile test is the most common experiment used to study the mechanics of cornea. In the tensile test, specimen is secured between two clamps which hold specimen tightly and prevent any sliding. One of the clamps is fixed and the other clamp applies displacement control or force control load to specimen through a driver. Tensile test is popular because in the in-vivo condition the intraocular pressure creates tensile forces in the cornea. There are several previous works on the tensile properties of cornea[20, 22, 27, 28].

In the following, we review some of the previous work which used uniaxial tensile experiments for characterizing corneal mechanics. Elsheikh et al[17] performed uniaxial tensile test on the human and porcine corneas. The result show that the human cornea at two different rates and ages is stiffer than porcine cornea. Boschetti et al[22] assessed steady state and stress relaxation behavior of porcine cornea for multistep load applying. They also reported Elastic modulus and Poisson's ratio of porcine cornea. Kampmeier et al[28] reported effect of temperature on biomechanical response of cornea in tension and stress relaxation tests. Their results indicated that temperature raise stiffens the cornea and reduces extensibility. Kaplan and Bettelheim[29] has studied the dynamic properties of bovine cornea. In their study, loss modulus, storage modulus, and tan(δ) were measured in the temperature sweep test.

The previous studies showed a wide variation in the measured stress-strain behavior and stiffness of cornea. One goal of this thesis is to provide new possible explanations for the existing wide variation in the reported corneal tensile behavior. The proper characterization of material properties is essential for developing more accurate computational models to predict corneal mechanical behavior.

2.3. Riboflavin/UVA Crosslinking Treatment

Keratoconus is a progressive non-inflammatory stroma thinning disorder. The previous investigation estimated that from every 100,000 people, about 55 persons have this disease[30]. The reported data showed that Keratoconus corneas have significantly lower stiffness comparing to normal corneas and show softer behavior under applied load[31-33]. Softening effect and change in corneal curvature impair the vision and light will not be

focused correctly on the retina. In this disease, patient will not become blind because of Keratoconus, but clear and correct vision loss are common consequences[30].

Corneal crosslinking is a new introduced method for halting progression of Keratoconus and recovering corneal biomechanical properties[34-36]. There are many studies that have been examined the treatment in the in-vivo and in-vitro conditions to investigate various effects on corneal biomechanics and vision. Long term investigation mechanical properties of cornea after collagen crosslinking has shown 81% to 95.5% halted in Keratoconus progression[36, 37].

Hayes et al[38] stated in the crosslinking treatment, new bonds have formed within collagen molecules and proteoglycans and also between collagen molecules and proteoglycans. They concluded that this is the reason for increased stiffness and integrity of cornea ultrastructure. Immunofluorescene imaging showed that collagen fibers are condensed and organized after treatment and this effect is available in 182.5 µm crosslinked zone[39, 40], in Figure 2.7. Increased stiffness post-treatment enables cornea to retain the correct curvature for focusing the light on the retina[39-41].

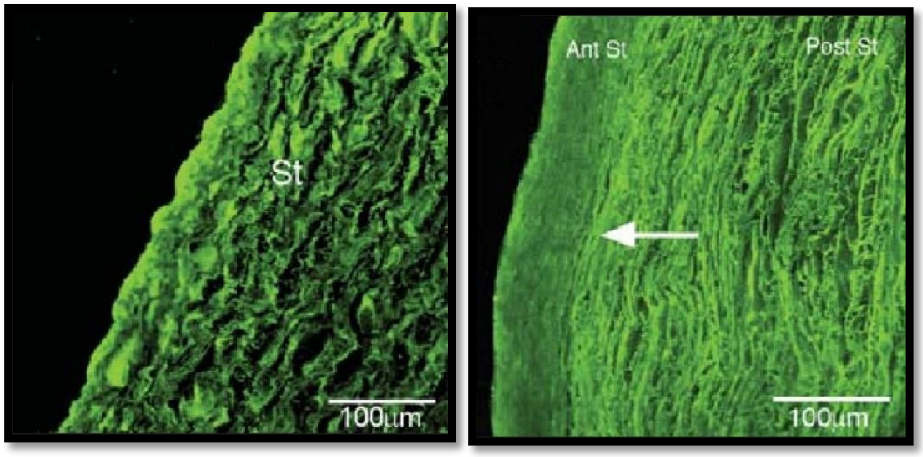

Figure 2.7. Immunofluorescence confocal microscopy of (Right) Control porcine stroma, and (left) Crosslinked porcine stroma. The collagen fibers become more dense and organized following collagen crosslinking[39].

Different mechanical testing methods have been used to obtain a comprehensive understanding of crosslinking treatment effects on the cornea. Søndergaard et al[42] reported that the crosslinking treatment improves the shear resistance of cornea in both anterior and posterior section of treated cornea[42]. Reduction in swelling pressure (the mechanical pressure applied to the surface to prevent swelling) was observed for the full thickness cornea and also anterior and posterior corneal flaps[43]. Kontasakis et al[44] did the indentation test on the cornea and stated there is no significant difference in compressibility (the slope of force versus deformation in the transverse direction) between crosslinked and control corneas.

Uniaxial tensile tests have also been used to study the crosslinking treatment. Wollensak et al[41] measured 328.9% and 71.9% increase in the applied stress to the treated human cornea and porcine cornea, respectively, comparing to the untreated corneas. McCall et al[45] reported 145% and 167% increase in the breaking strength of shark and rabbit crosslinked cornea, respectively. In addition, they have reported that crosslinked cornea using UVA

only or Riboflavin only does not have any significant effect on the breaking strength. Spoerl et al[46] examined the effect of UV wavelength on the biomechanical properties change. The results indicated that the stress strain behavior of porcine crosslinked cornea is stiffer when UV light with 365 nm wavelength is used that when 254 and 436 nm UV light is used. Wollensak et al[47] measured biomechanical response of crosslinked rabbit cornea immediately after treatment, after three months, and after 8 months. They reported 85% increase in rigidity of cornea and also no significant effect due to time of measurement.

In the current study, effect of collagen crosslinking treatment on the tensile stress, stress relaxation and dynamic properties of bovine cornea was measured. In addition, effect of water content of crosslinked cornea on the stress strain behavior and tangent modulus was examined.

Chapter 3

Materials and Methods

Research work presented in this thesis can be divided to the main five categories as shown in Figure 3.1.

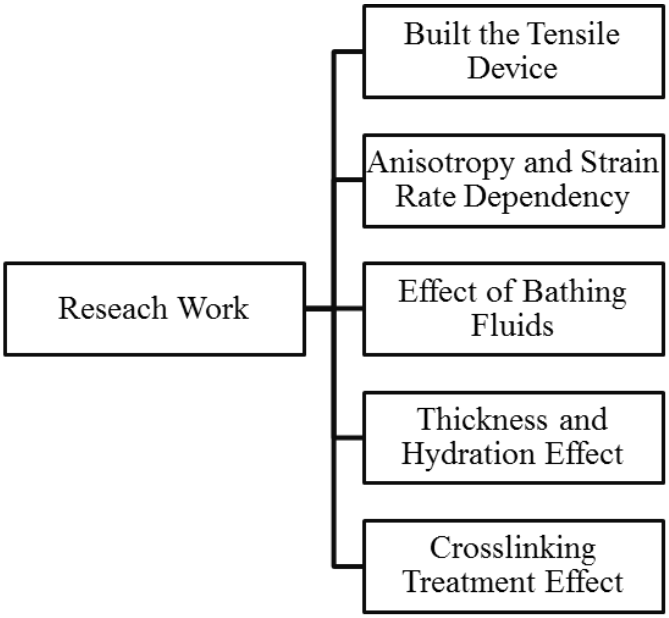

Figure 3.1.Summary of research works have been done in this thesis.

3.1. Sample Preparation

Fresh bovine eyes were obtained from local slaughterhouse. The enucleated whole eyes were transported on ice in plastic bags in a cooler. Intact eye globes with undamaged epithelium were chosen to dissect and used in the experiments. In a dissection pan, eyes

were dissected. Special care was taken to prevent any damage to cornea through dissection. First, using a sharp scalpel, a hole was created in the sclera and with a surgery scissor, a corneal scleral ring was obtained from each eye globe. The custom made double bladed parts were built to punch strips including 2-3 mm of sclera with 3 and 5 mm width. The IS and NT directions were determined based on the shape and dimension of whole eye globe. Strips were cut in the IS and NT directions to use in different sets of experiments. Some of the samples were used for the tensile test at the same day and others were wrapped in a cling film and kept in -80^{o}C freezer. Prior to the experiments, frozen specimen was let to thaw for 15 minutes. Five corneal stromas were tested in each category.

3.2. Tensile device

To study the mechanical properties of the cornea in the tension, we built a tensile testing device. Previous designs were reviewed and strengths and drawbacks of each designs were analyzed. In addition, based on the previous reports, the required specifications which were necessary for doing uniaxial tensile test on the soft connective tissues were collected. It was tried to achieve to the best design to satisfy both mechanical standards and test requirements.

The tensile test on the cornea should be done in the submersion chamber to simulate the physiological condition. Therefore, it was a main criteria to design the device in order to have a chamber that can be filled with the proper solution. Designing clamps that can hold the sample tightly and ensure good gripping was another important step. For this purpose, it was decided to serrate both top and bottom clamp plates, so the sample was secured completely and it prevented any slippage as shown in Figure 3.2.

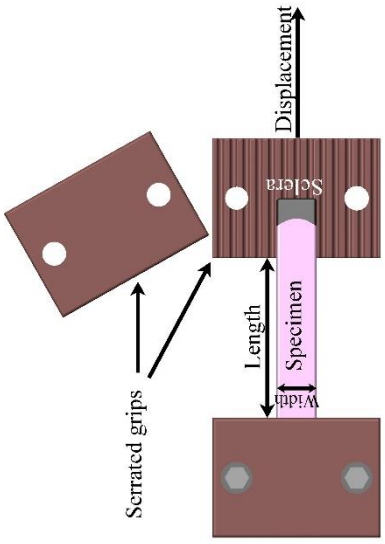

Figure 3.2. The grips were serrated to prevent any slippage.

By reviewing the previous designs and assessing type of our experiment's requirements, it was a better choice to design and assemble the tensile device horizontally instead of vertically. One advantage of this setup is that if there is any vibration because of stepper motor, the continuous contact with ground will absorb the vibration and prevent any noise in the measurements. In the horizontal setup, one side should be fixed and the load is applying from the other side. Choosing the appropriate driver and load cell was left for after finalizing the design. Based on this findings, the initial setup was designed as shown in Figure 3.3.

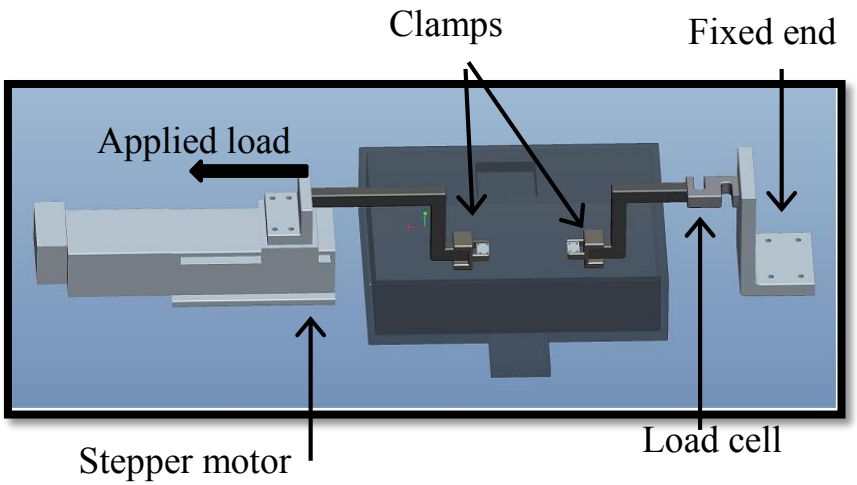

Figure 3.3. Initial design of uniaxial tensile device based on the requirements

The range of possible load that may apply to the cornea in the tensile test was estimated. Using the force data and analyzing different applied stress, the connections between motor and clamps and between clamps and fixed end were determined. When assessing the possible stresses and moments in the design accurately, one deficiency was found. The weight of arm and the clamp that was connected to the load cell applied significant moment to the load cell. The moment could affect the measured force value. Therefore, the load cell position was moved next to the clamp and with further analysis of stress at different points of device, the design was finalized as shown in Figure 3.4.

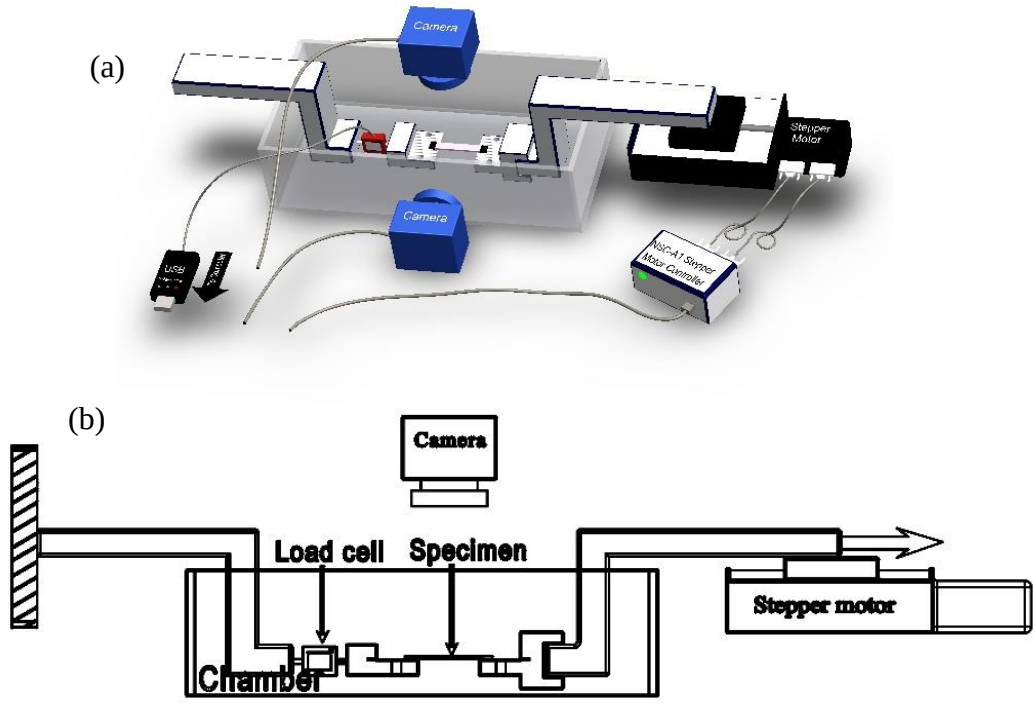

Figure 3.4. (a) Isometric view, (b) schematic plot of modified uniaxial tensile device design. Two cameras were added to measure the thickness and width during the experiment (In part (b), the horizontal camera was deleted for clarity.).

Measuring thickness and width during the experiments provided beneficial data for the deformation and swelling behavior of cornea. For this purpose, it was decided to install two cameras horizontally and vertically, Figure 3.4(a).

Since, it was our goal to conduct displacement rate dependency of specimen, a displacement control stepper motor was selected to use in the device. A stepper motor (Precision Linear Stage NLS4, NEWMARK SYSTEM INC., California, USA) with the resolution of 0.13 µm which was made of light and stiff Aluminum (6061) with a stainless steel lead screw was chosen. A smooth motion with a good load capacity was achieved with linear guide bearing. The stepper motor was connected to a stepper motor controller

(NSC-A1, NEWMARK SYSTEM INC., California, USA). The motor controller consisted of a micro stepping driver and a programmable controller and an assigned software (NSC-A1) was used to program the motor movement. In the below, written code for preconditioning procedure discussed in chapter 3 is presented:

```
HSPD=656
LSPD=10
ACC=2
EO=1
V2=-87609
V3=V2/10
V4=V2+V3
V5=0
WHILE V5<5
XV4
XV2
V5=V5+1
ENDWHILE
HSPD=1312.4
V5=0
WHILE V5<3
V5=V5+1
XV4
WAITX
DELAY=60000
XV2
WAITX
DELAY=30000
ENDWHILE
END
```

Recording force data was done by means of a 22N submersible load cell (Submersible S-Beam Load Cell LSB210, FUTEK INC., California, USA) connected to a USB interference (USB215, FUTEK INC., California, USA). This digital interference between computer and load cell was responsible for analog to digital data conversion, filtering, and transmitting data to computer. Collecting data was done by SenseIT Test and Measurement software (Ver.2.1.4, FUTEK INC., California, USA). The load cell was calibrated for the tension

forces by company. Maximum system error was 0.2% of output. In addition, after a year, the load cell was sent back to the company for re-calibration.

Stress analysis showed that Aluminum is a proper choice for the connections between clamps and motor, and between load cell and fixed end. The Aluminum was also used for building clamps. In addition, light weight and corrosion resistance of Aluminum were other properties that makes it the best choice. For assembling the different parts of device, an Aluminum breadboard stage was built. Clamps, breadboard stage, and arm connections were built in DML (Design and Manufacture Laboratory, Oklahoma State University).

A microscope (H800, American Scope, Irvine, California, USA) which used a 10 megapixel camera (MU1000, American Scope, Irvine, California, USA) to take images was connected to a desktop computer with the USB connection. Since, it was hard to align a big microscope in the horizontal direction, an USB digital microscope (26700-300 ZipScope microscope, Aven Inc., Michigan, USA) was used to take images of the specimen's thickness. Image analysis toolbar of MATLAB (Natick, Massachusetts, US) was used to calculate the thickness and width of specimen by counting pixel data. A plastic specimen with 5 mm width and 1 mm thickness was used as reference for measuring thickness and width. It was also notable to mention that using these images, the length of specimen was calculated and compared with measured length from stepper motor. The finding showed that measured length by stepper motor is accurate with less than 1% error.

Considering all of discussed issues, the device was built and assembled, see Figure 3.5. To calibrate the device and be certain about precision and accuracy of device, tensile test on the bovine stroma was done using the similar test conditions as Boyce et al[27]. The specimen

was cut in the NT direction and immersed in OBSS. Pre-conditioning was also applied prior to the experiments. Results in the Figure 3.6 show that obtained result from our device is in good agreement with reported result by Boyce et al[27].

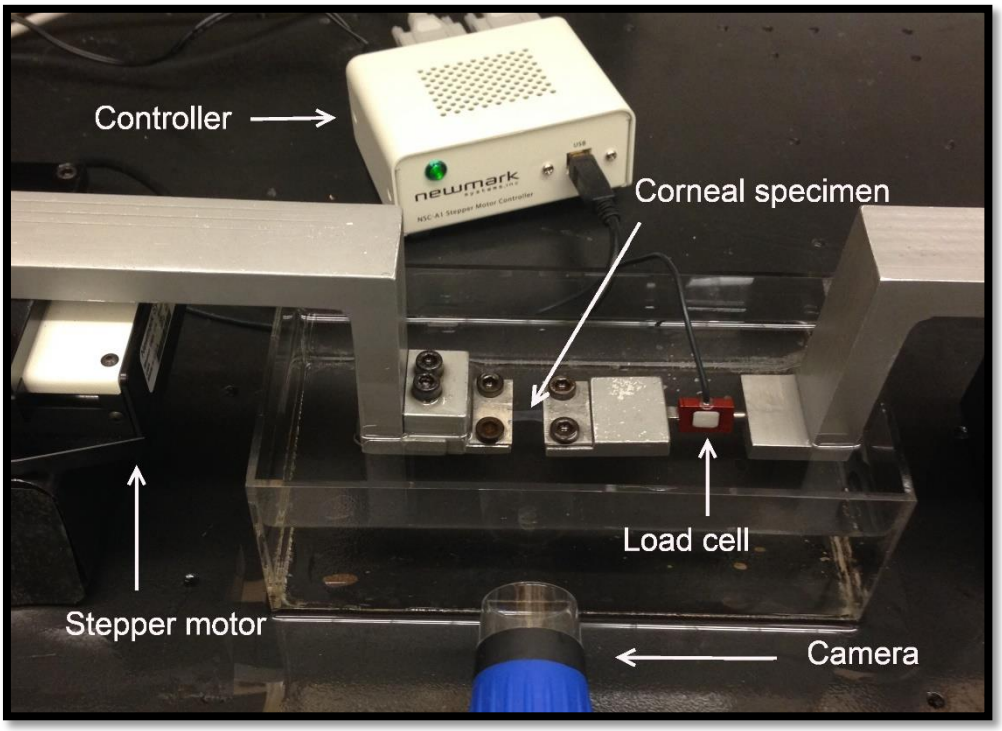

Figure 3.5. Picture of the custom built tensile device including microscopes for measuring thickness and width of specimen

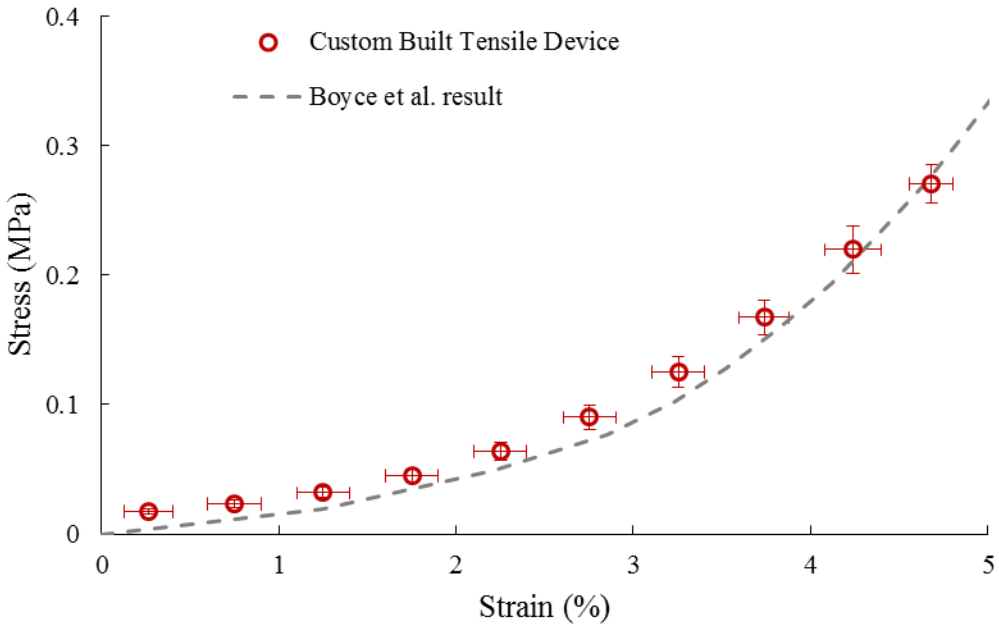

Figure 3.6. Stress strain behavior of bovine cornea under tension and comparison with Boyce et al's result.

3.3. Test procedure

Pre-conditioning was applied prior to the test, to achieve a recoverable state and remove the initial slack. Few previous work on corneal mechanics has applied preconditioning[27, 28, 48, 49]. The preconditioning procedure consisted of 5 loading/unloading cycles with 5 mm/min speed and 3 subsequent stress relaxation steps using 10 mm/min speed for the ramp section to 10% strain, see Figure 3.7(a). A normalized force time response of preconditioning is shown in Figure 3.7(b). After pre-conditioning, the sample was let to recover for the 5 minutes. A preload about 100 mN was applied to straighten the strip and ensured that the sample was under tension[22, 27, 48]. Initial length was the length of sample after applying 100 mN. Purpose of pre-conditioning is to remove initial slack and establish a reference state for testing mechanical properties.

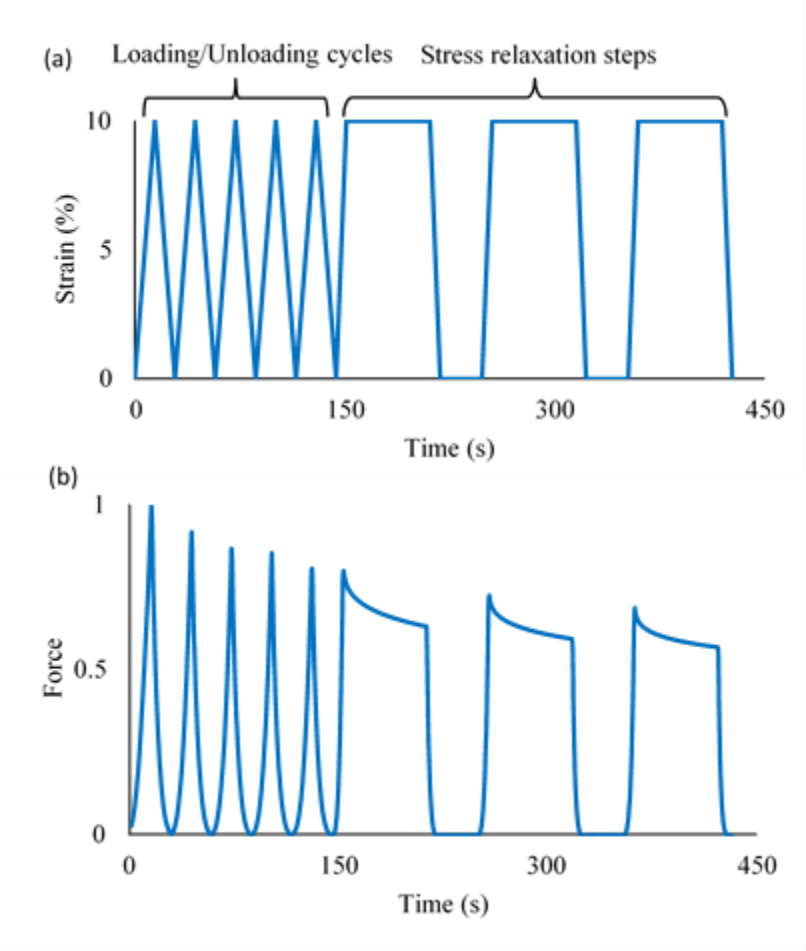

Figure 3.7. (a) Preconditioning procedure which has been applied before tensile experiment, (b) A normalized force time response of bovine cornea in preconditioning.

Stress was defined as the force divided by the cross section area of the strip. The cross section was calculated after pre-conditioning and before starting the test using the images from two microscopes. Axial strain was defined as elongation divided by the initial length.

3.4. Anisotropy and Strain rate dependency

Due to time issues, some of specimens were frozen and used later. To examine the effect of freezing on the mechanical behavior of strips, five fresh and frozen NT strips were tested in 0.9% NaCl using 2 mm/min displacement rate.

To study the effect of the strain rate on the mechanical behavior of bovine strips, uniaxial tensile tests were done under wide range of displacement rates. The strips were preserved in the saline solution until thickness reached about 1.1 mm. Tests were done on the NT strips in 0.9% NaCl solution using low rates,1 and 2 mm/min, to high rates such as 5 and 9 mm/min displacement rates.

As discussed earlier, collagen fiber distribution is not similar in all directions. To study anisotropic property of cornea, uniaxial tensile tests were done on IS and NT bovine strips. They were conducted with 2 mm/min speed in 0.9% NaCl on the strips with thickness about 1.1 mm.

3.5. Effects of bathing solution on tensile properties

To observe the effect of swelling on the biomechanical properties, tensile tests were done in different bathing fluids. Distilled water, 0.9% NaCl, 12% NaCl, Phosphate buffer saline (PBS) (AMRESCO LLC, Ohio, USA), Mineral oil (Fisher Science Education, Illinois, USA), Ophthalmology balanced salt solution (OBSS) (ALCON laboratories, Inc., Texas, USA) were used as a bathing fluids in the tensile test on the bovine NT strips. The thickness was measured after recovery time in preconditioning and before starting the test. The whole preconditioning and recovery time let strips to reach to an approximate equilibrium state of swelling. Following the ramp section, the sample was held at the fixed strain and force relaxation was collected for 2000 seconds.

3.6. Relation between thickness and mechanical behavior

In order to consider the relationship of stress strain behavior and viscoelastic response of cornea with thickness change, strips with different thicknesses were tested. Six groups of thicknesses were chosen from 400 µm to 1500 µm. Displacement rate was 2 mm/min and mineral oil was used as a bathing fluid. Stress relaxation was done as described before. Mineral oil was chosen because it has been reported that hydration change in mineral oil is negligible[20, 50, 51]. Under the same conditions, 5 NT strips with 3 mm width were tested to observe failure curve. These samples were stretched up to the failure point.

Since, elastic modulus of connective tissues are changing with strain change, it is not true to ascribe one specific young modulus to the tissue[52, 53]; therefore, various equations like power and exponential formulas are used to fit the experimental data. By finding, the material parameters in the formulas, elastic modulus can be calculated at each desired strain. These formulas have been used widely to define stress-strain behavior of soft tissues in different experiments, like tensile test on skin[54], muscle[55], and tendon and ligament[56-58].

By curve fitting the experimental data, the unknown parameters were determined and analyzed. Initially, the exponential law was suggested to fit the experimental data from inflation and compression tests on the cornea[50, 59],

$$\sigma = A(e^{B\epsilon} - 1) \quad (1)$$

A and B are the material parameters that will be found after curve fitting to the experimental data. The power formula has been used to fit to the uniaxial tensile test on the cornea[49],

$$\sigma = \alpha(\epsilon - \epsilon_0)^{\beta} \quad (2)$$

where α, and β are constant to be determined after fitting. Curve fitting Tool in Matlab (Natick, Massachusetts, US) was used to curve fit the experimental data.

3.7. Riboflavin/UVA Crosslinking Treatment

The desired solution for crosslinking treatment is 0.1% Riboflavin solution which is made of 10 mg riboflavin-5-phoasphate sodium salt dihydrate (Alfa Aesar, Massachusetts, USA) in 10 ml of 20% dextran T-500 (Spectrum, California, USA). Using high molecular weight dextran does not let the cornea to swell. The frozen specimen was let to thaw for 15 minutes. The scleral corneal ring was placed in 0.1% Riboflavin solution and kept in 4 ºC to minimize evaporation until the specimen's swelling reaches to the equilibrium. The equilibrium was determined when the difference between thickness measurements in 30 minutes period became less than 10% of the corneal thickness. It usually takes up to 2 and 3 hours to reach swelling equilibrium. The average thickness of specimens were between 700 to 800 µm. Pachymeter (DGH Pachette 3, DGH Technology, Inc., Pennsylvania, USA) was used to measure the corneal thickness. In the treatment process, the specimen placed on a half wooden sphere to present the same shape as eye globe, Figure 3.8. For radiation source, two UV lEDs with 365 nm wavelength (Roithner lasertechnik GmbH, Vienna, Austria) were used with a resistor in series. The resistor was chosen in order to have intensity of 3 mW/cm^2 in the 2 mm distance of led. The UV light was radiated to cornea for 30 minutes and every 5 minutes drops of riboflavin solution was added on the cornea surface. Specimens categorized into two groups based on the type of treatment:

Group 1: Control specimens were tested without any Riboflavin/UVA treatment

Group 2: Corneas crosslinked while UV light radiated to the anterior side.

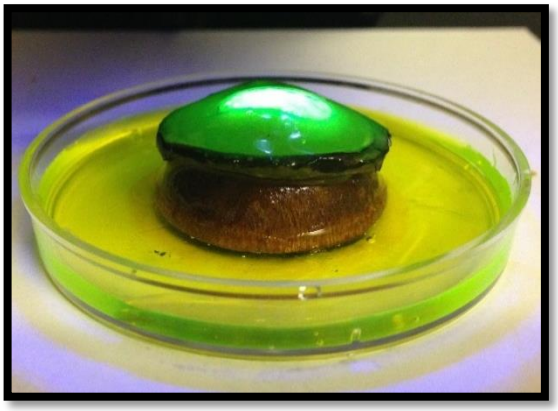

Figure 3.8. The corneal scleral ring was placed on a half wooden sphere to present the same shape as eyeglobe.

3.7.1. Uniaxial tensile test

After the crosslinking treatment, a strip was punched with 5 mm width from each corneal sclera ring in the NT direction. The specimen was placed in the OBSS for 15 minutes prior to the experiments. Dynamic mechanical analyzer (DMA) (RSA-G2, TA instrument, Delaware, USA) was used to conduct uniaxial tensile and dynamic tests. Specimen was secured between two clamps and sand paper was used on the clamps to prevent slippage of cornea. An immersion chamber was used to conduct experiment in the OBSS solution. Preconditioning was done using the discussed procedure. Test started with applying 5% uniaxial strain using 5 mm/min displacement rate and 1200 seconds stress relaxation following.

Effect of hydration and thickness change on the mechanical properties of collagen crosslinked cornea was studied. One objective of this work was to measure that how the

water content of cornea affects the observed increased stiffness after collagen crosslinking. For this purpose, three thickness groups (700, 1100, and 1500 μm) were chosen and uniaxial tensile and stress relaxation tests were done. The mechanical testing was conducted in mineral oil and using 2 mm/min displacement rate. For the control group, the results from the previous section was used.

3.7.2. Dynamic tensile testing

To assess dynamic properties, specimen is subjected to a sinusoidal uniaxial strain,

$$\varepsilon(t) = \hat{\varepsilon}\, exp(i\omega t) \tag{3}$$

where, ε represents amplitude of applied strain and ω is the angular frequency. When amplitude of applied strain is small, it can be assumed that the stress response is in the linear viscoelastic region[52], so the tensile stress response, as shown in *Figure 3.9* may be defined as,

$$\sigma(t) = \hat{\sigma}\, exp(i\omega t + \delta) \tag{4}$$

where, δ and $\hat{\sigma}$ are the phase shift and amplitude of stress response, respectively. For an elastic material, phase shift will be zero and for a pure viscous material, it will be equal to 90º. For other materials, the value falls between zero and one. The stress, σ(t), can be decomposed into two components; one in phase, the other out of phase from the input strain. The measured stress response is the summation of the two waves, and one can writes,

$$\sigma(t) = \sigma'(t) + \sigma''(t) = \hat{\sigma}' Sin\, \omega t + \hat{\sigma}'' Cos\, \omega t \tag{5}$$

where σ' and σ'' can be expresses as,

$$\sigma'(t) = Im\{\hat{\sigma}' e^{i\omega t}\} \quad , \quad \sigma''(t) = Re\{\hat{\sigma}'' e^{i\omega t}\} \tag{6}$$

The complex modulus E^* has two components, storage modulus and loss modulus. Storage modulus, E', is the elastic component which stands for elastic energy saved in the material and this energy can be recovered. Loss modulus, E'', is the viscous component that presents energy dissipated by material. The complex modulus can be written as,

$$E^*(\omega) = \frac{\sigma}{\varepsilon} \quad , \qquad E^* = E' + iE'' \tag{7}$$

The phase shift (tan(δ)) may be defined as the ratio of loss modulus to storage modulus which shows ability of material to damp the energy,

$$\frac{E''}{E'} = \tan(\delta) \tag{8}$$

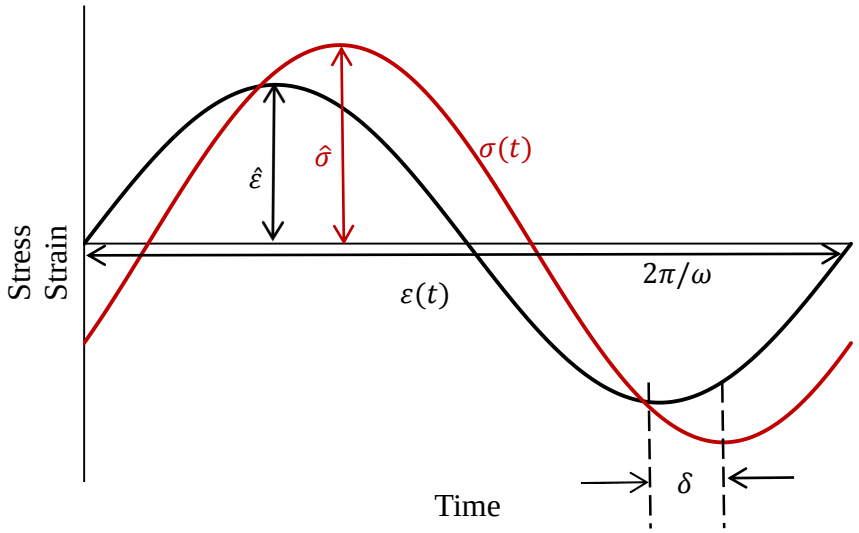

Figure 3.9. Applied sinusoidal strain and measured stress response and also showing measured parameters

After uniaxial tensile test and relaxation step, a frequency sweep test was conducted from 0.01 to 20 Hz with 0.1% strain amplitude. At each frequency, two cycles were done as preconditioning and the average data from the next three cycles were used.

Preliminary strain sweep tests (results are not presented here.) were done to determine the correct strain amplitude for frequency sweep. In this test, the oscillating strain amplitude increased from 0.005% to 5% strain using 0.1, 1, and 10 Hz frequency. The region in which storage modulus was not dependent on strain amplitude was 0.005% to 0.2% strain; 0.1% was chosen as strain amplitude for frequency sweep. Conducting strain sweep test and finding the region that storage modulus is strain independent is a requirement for linear viscoelastic theory.

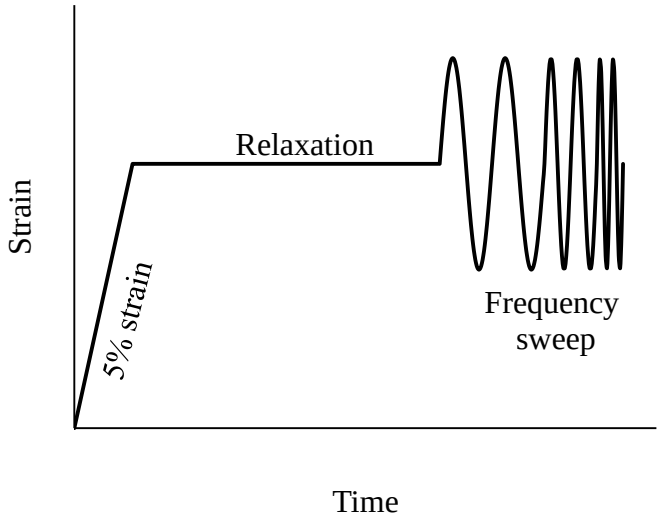

Figure 3.10. Test procedure for the uniaxial tensile, stress relaxation, and dynamic tests (Amplitude of frequency sweep is 0.1% strain, but to have a better view, the curve is not plotted on scale).

3.8. Data Analysis

One way ANOVA test was used to examine change in mechanical properties of different groups. The level of significance was set at 0.05 in all of statistical analysis.

Chapter 4

Results and discussion

4.1. Anisotropy and strain rate dependency

In the tensile test, different properties of cornea can be studied. In this chapter, stress strain response, tangent modulus, stress relaxation, and dynamic properties will be discussed. Because sample preparation and conducting experiments are a time consuming process and also high number of experiments was done, it was not feasible to run all of experiments on one day, so some of specimens were frozen. To assess the effect of freezing on the obtained results, mechanical properties of fresh and frozen cornea were compared in the tensile test. Figure 4.1 compares the stress strain behavior of fresh and frozen strips. The figure shows that freezing process does not have any significant on the mechanical properties ($P < 0.05$). It has been reported that the freezing does not have significant results on swelling and viscoelastic properties of soft tissues[60, 61].

Uniaxial stress strain curves from different strain rates are plotted in Figure 4.2. This figure confirms that the cornea is strain rate dependent and in the higher strain rates, cornea shows stiffer behavior.

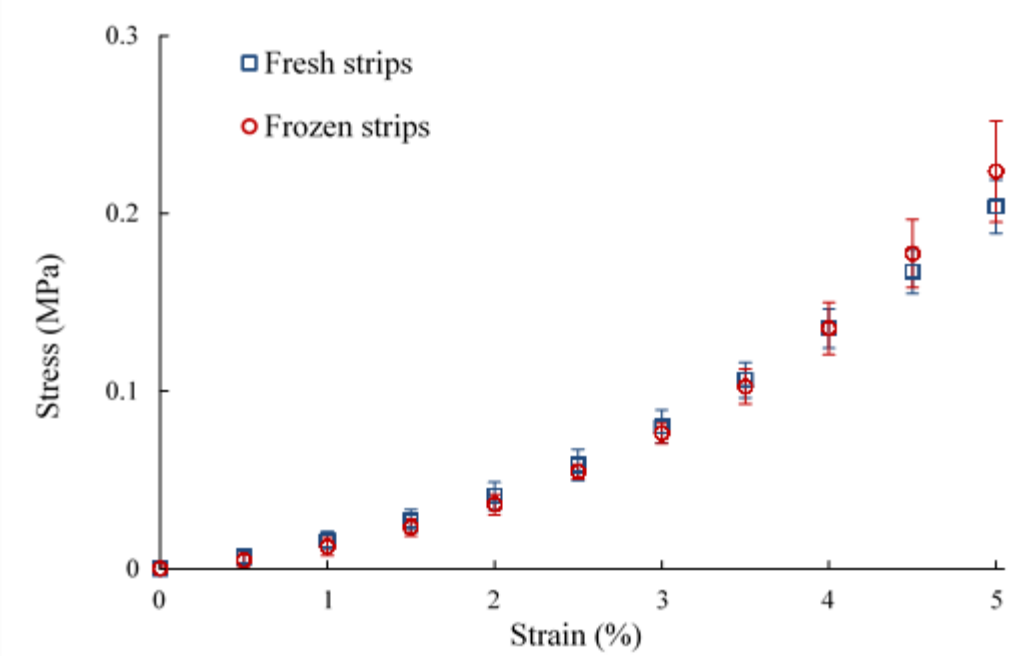

Figure 4.1. Stress strain behavior of fresh and frozen strips. The figure shows that freezing process does not have significant effect on the mechanical properties ($P < 0.05$) (Error bars show the standard deviation in the average stress).

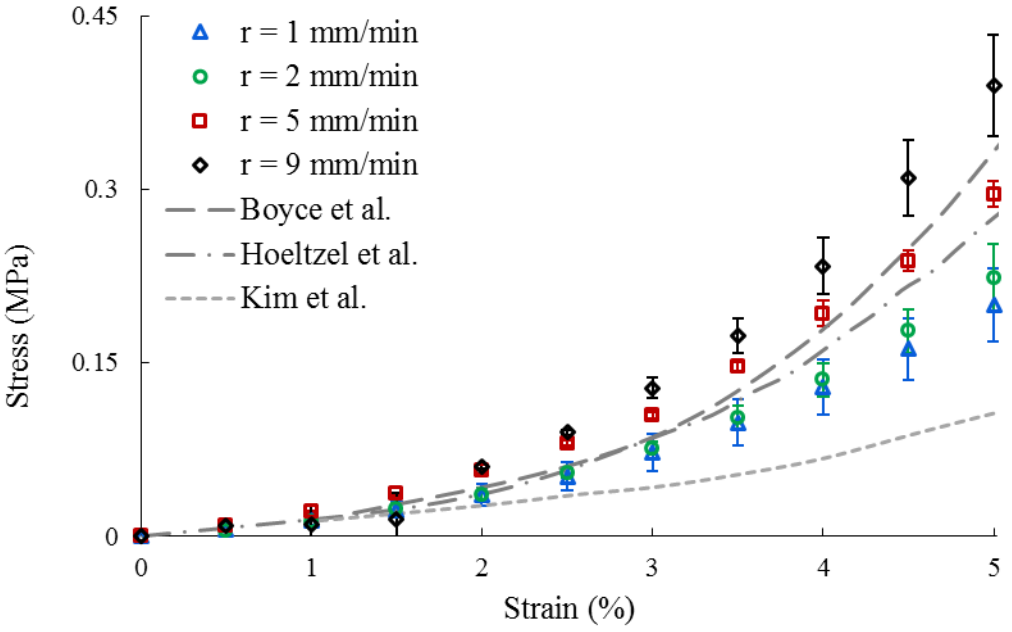

Figure 4.2. Uniaxial stress strain curves from different strain rates. The measured stress was same almost for different strain rates up to 2% strain. As the strain increased, the results became rate dependent.

Corneal mechanical properties highly depend on the extracellular matrix and collagen fibers. Extracellular matrix is a ground substance for the collagen fibers which are distributed with specific orientation. Matrix mechanics is vital to preserve structural integrity of cornea. However, small portion of tensile load bears by matrix, degenerated matrix weakens the cornea significantly. Collagen fibers are the load bearing element in cornea and they have nonlinear response to the applied load. Depend on the orientation of fibers relative to applied load, the response varies. When the fiber direction is parallel to the applied load, the fiber shows the stiffer behavior.

Strain rate sensitivity of bovine corneal stroma is related to the viscoelastic deformation of collagen fibrils in response to the applied load. In the higher rates, collagen fibrils does not have enough time to reorient to the applied load direction, so higher number of fibrils will be under tension. Previous reports have also observed strain rate dependency for tissues like, skin, bone, and tendon[56, 62, 63]. In Figure 4.2, results of previous studies[27, 49, 64] are presented for the comparison. The obtained result in the current study is in good agreement with the experimental data presented by Boyce et al[27] and Hoeltzel et al[49]. The lowest rate that was used in the current study was 1 mm/min (0.14%/s) which is very close to the 0.16%/s rate which Kim et al[64] used. Kim et al[64] did not use preconditioning for their samples. This could be a possible reason for why our results do not match theirs. Boyce et al[27] have done tensile tests without preconditioning and they observed the same behavior as Kim et al's data[64]. Preconditioning is used in the current study to attain a reference state and remove inelastic strain.

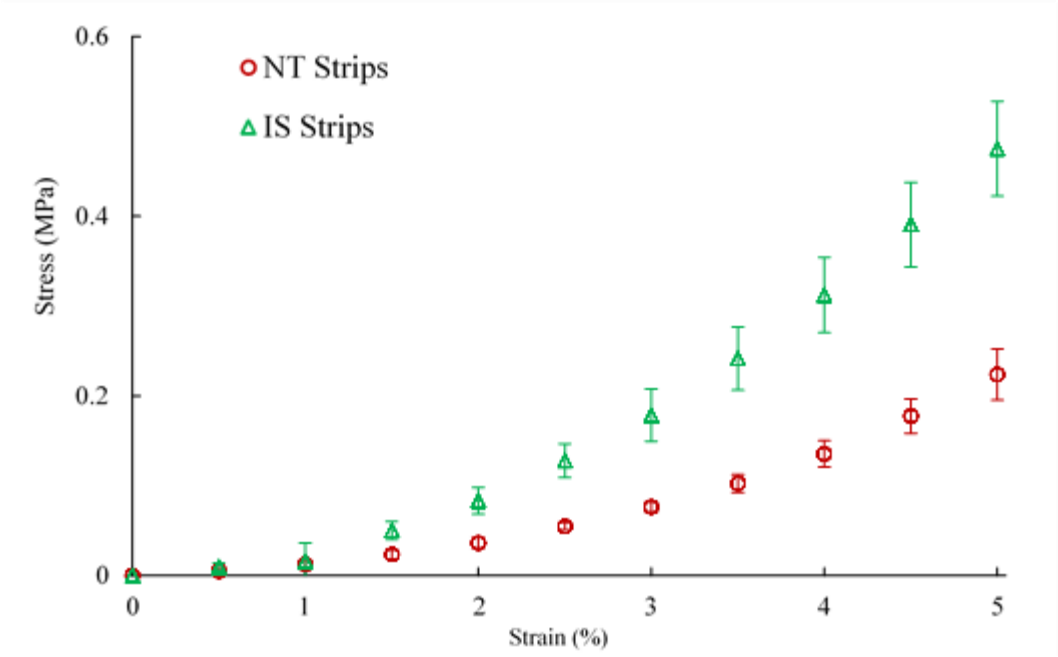

Figure 4.3. The result depicts that the IS bovine strips are much stiffer than NT bovine strips.

NT and IS strips were tested to investigate the difference between collagen distribution in the horizontal and vertical directions. The result in Figure 4.3 depicts that the IS bovine strips are much stiffer than NT bovine strips. The same trend has been reported for porcine corneas[17, 22, 28]. Collagen fibrils for bovine cornea are mainly arranged vertically (IS direction) and circumferentially[16], Figure 4.4. The measured stress strain responses for NT and IS directions are in good agreement with reported data from WAXRD in Figure 4.4; Therefore bovine cornea is stiffer in the IS direction because of higher fiber density and preferred orientation of collagen fibrils.

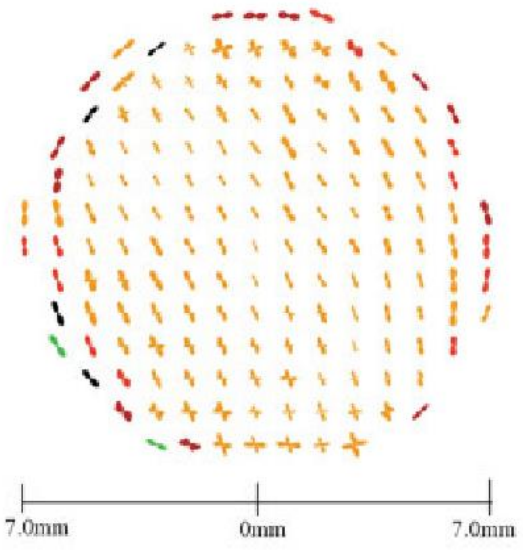

Figure 4.4 Vector plot map shows that stromal collagen in the bovine cornea is orientated mainly in the 30 degrees from vertical axis[16].

4.2. Effects of bathing solution on tensile properties

Characterizing mechanics of cornea has been the goal of many studies which resulted in a wide range of values for mechanical properties. Young's modulus of cornea are reported in the wide range of 0.01 to 42 MPa[22, 65, 66]. Wide range of reported data can have different reasons. Variation in age, species, and experimental set up are known parameters that affect the measured values. Effect of hydration and bathing fluid are the possible causes that has not been considered to have an influence on the results. Swelling of cornea is not similar in different bathing fluids and mechanical behavior changes accordingly. In the current study, different bathing fluids were used in the uniaxial tensile test to assess how swelling affects the mechanical properties of cornea.

Thickness was monitored throughout the experiment and measurement are shown in Table 4.1. The thickness hydration relation for bovine cornea is[67],

$$t = 295\ e^{0.27\ H_w} \quad (9)$$

where t is thickness in μm and H_w is the hydration. Swelling rate was defined as the percentage increase in the sample thickness 10 minutes after tensile test. Stress strain behavior of strips in the bathing fluids is shown in Figure 4.5(a). As the swelling of the bovine cornea increases, the extensibility increases, too. Swelling also affects stress relaxation responses and the relaxed stresses are not similar in different bathing fluids, Figure 4.5(b). Figure 4.5(a) also compares obtained result with previous reported data[27, 49]. Because the thickness is not same for all strips, it may be claimed that the difference in stress is an artifact because of cross section difference. As shown in Figure 4.6, there is a similar trend in the force strain behavior which confirms that swollen cornea extends more at the same strain range.

Table 4.1. Average measured thickness and hydration using two microscopes and calculated thickness change rate.

Bathing Fluids	Before tensile test (μm)	10 min after ramp (μm)	Swelling rate (%)
Distilled water	2.00 ± 0.14	2.33 ± 0.21	16.76
PBS	1.34 ± 0.07	1.41 ± 0.06	4.90
0.9% NaCl solution	1.32 ± 0.04	1.39 ± 0.03	4.87
12% NaCl solution	1.04 ± 0.04	1.09 ± 0.04	4.09
OBSS	1.03 ± 0.06	1.08 ± 0.05	4.20
Mineral oil	0.70 ± 0.02	0.70 ± 0.02	~0.00

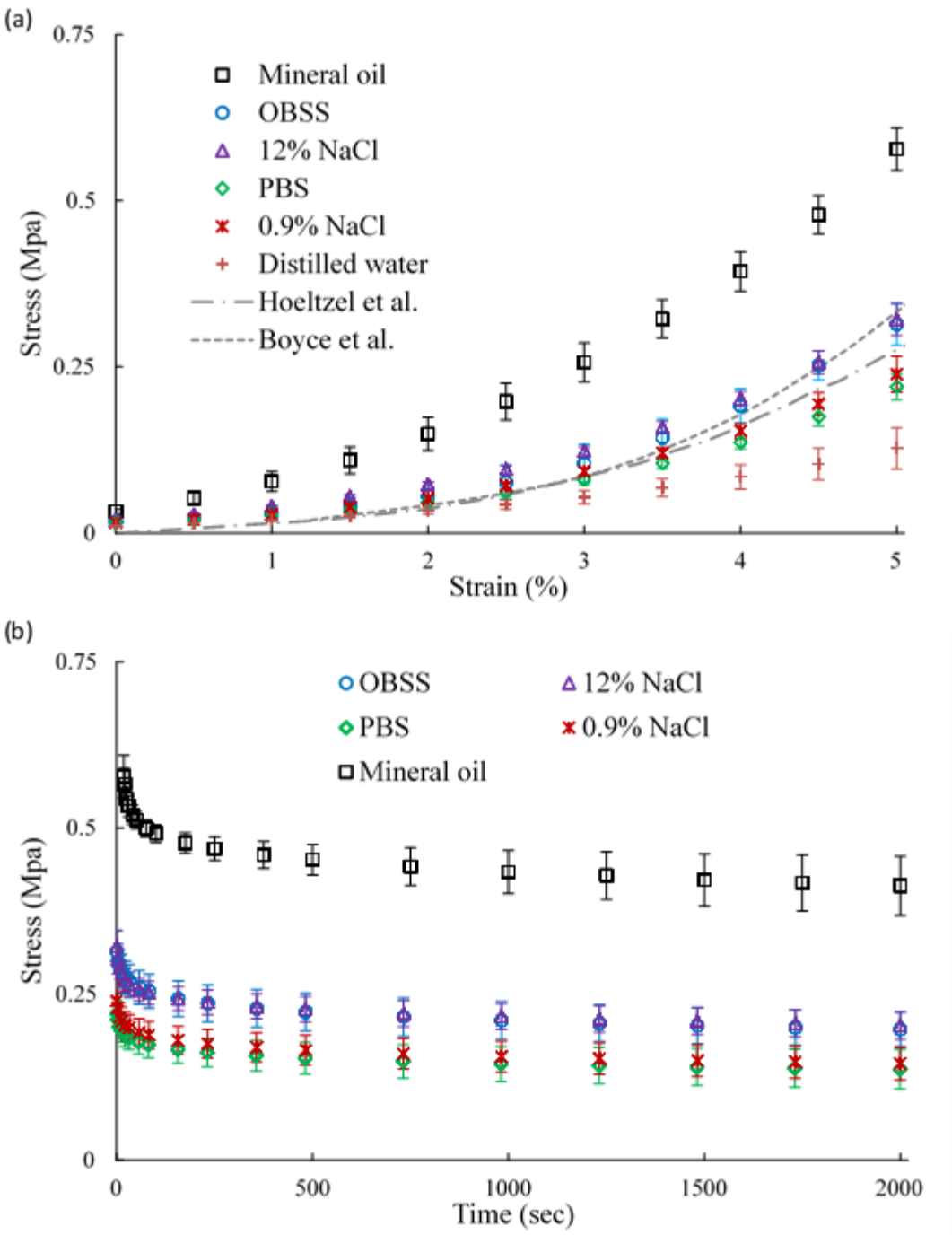

Figure 4.5. (a) Stress strain behavior of strips in bathing fluids and also comparing obtained result with previous reported data by Boyce et al. and Hoeltzel et al. (b) Stress relaxation response of strips in bathing fluids.

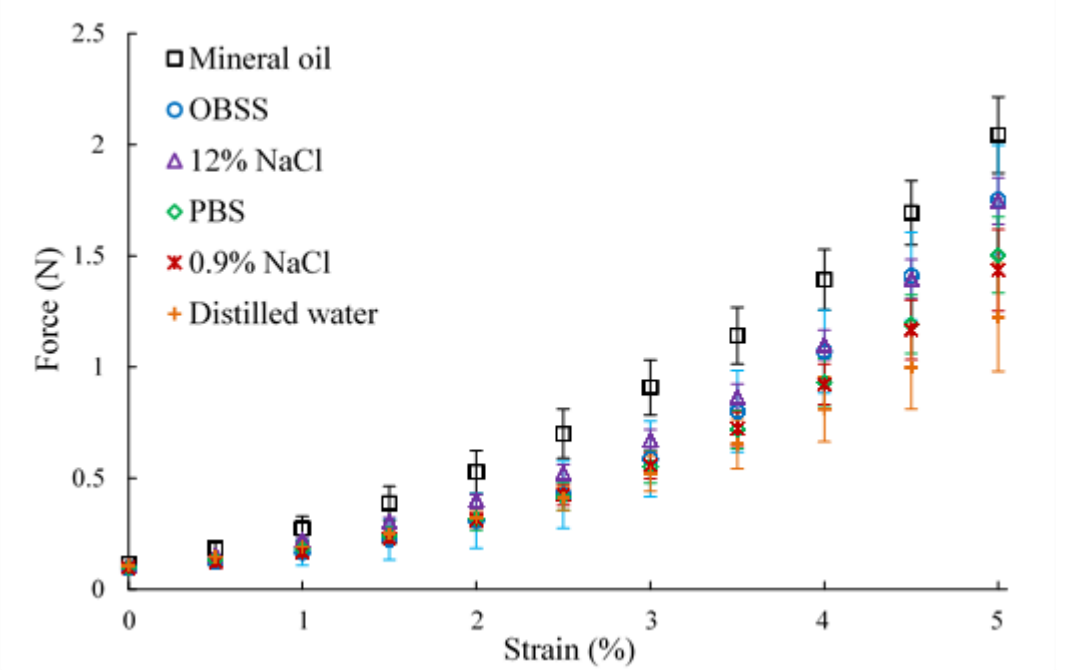

Figure 4.6. Force strain behavior of strips incubated in bathing fluids. Similar trends as stress strain behavior is observed.

Tangent modulus, hydration, and thickness for bathing fluid groups at 5% strain are presented in Figure 4.7. Statistical analysis depicted that tangent moduli of both PBS and 0.9% NaCl solution and both OBSS and 12% NaCl solution are not statistically different ($P < 0.05$). However, between other groups, there is a significant difference ($P > 0.05$). Maximum tensile stress and equilibrium stress in relaxation of 2000 seconds are displayed in Figure 4.8. Relaxation percentage for each bathing fluid group is calculated in Figure 4.9. Relaxation percentage was defined as the reduction in stress after 2000 seconds divided by stress at 5% strain.

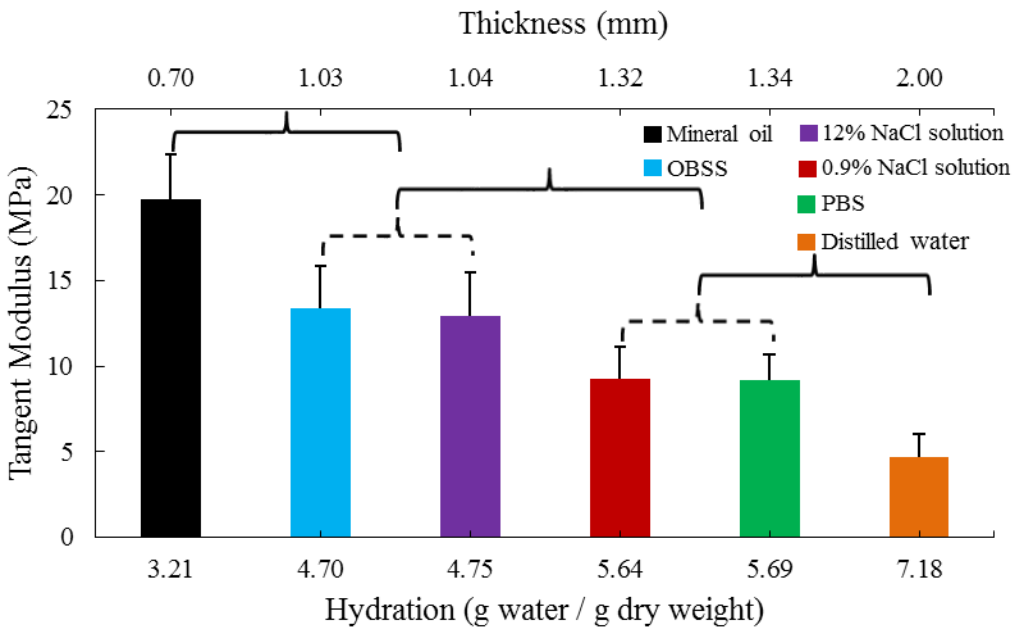

Figure 4.7. Tangent modulus, hydration, and thickness relation for bathing fluid groups at 5% strain (Bracket with solid line shows significant difference between groups ($P > 0.05$) and bracket with dash line shows that two group are statistically similar ($P < 0.05$).).

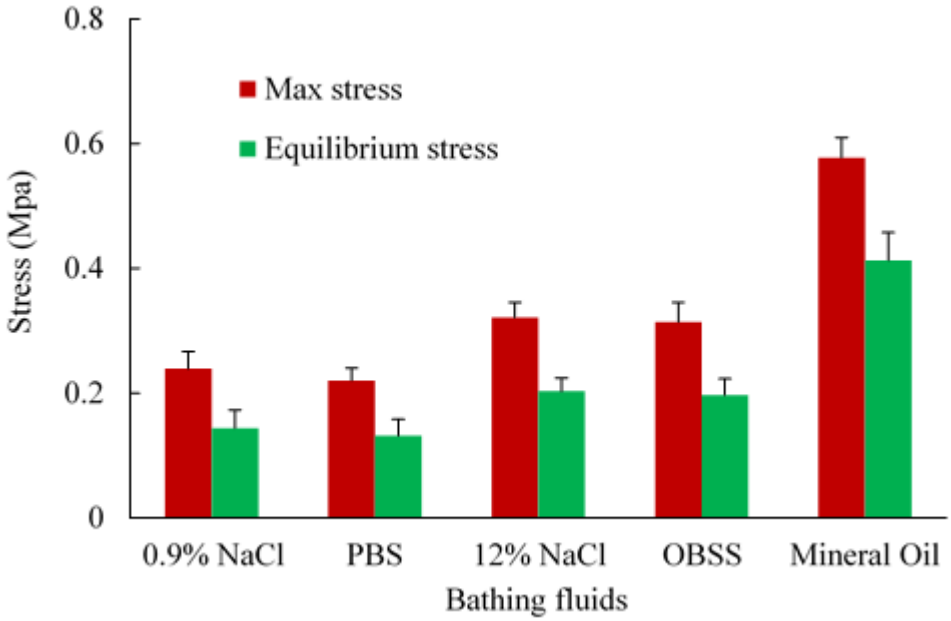

Figure 4.8. Maximum stress at 5% strain in tensile stress and equilibrium stress in relaxation after 2000 seconds for bathing fluid groups.

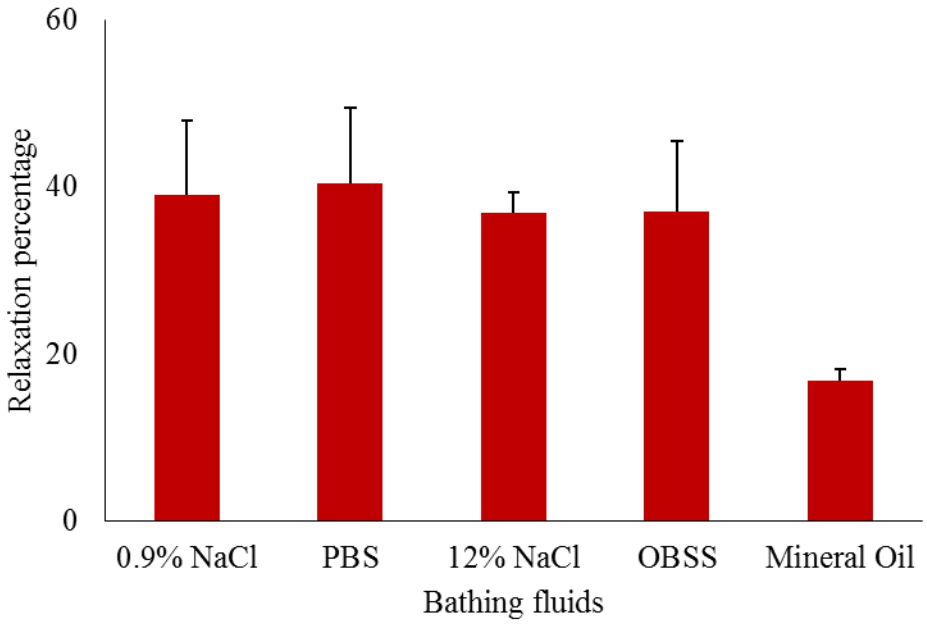

Figure 4.9. Relaxation percentage for each bathing fluid groups. As the cornea swells more, the cornea relaxes more.

An increase in hydration causes decrease in tangent modulus, in Figure 4.7; therefore, there is a negative correlation between tangent modulus and hydration. Tangent moduli of corneal strips in OBSS and 12% NaCl solution were statistically similar ($P < 0.05$) and the same between 0.9% NaCl solution and PBS ($P < 0.05$); while, the tangent moduli of strips incubated in mineral oil were significantly higher than those in OBSS and 12% Na Cl solution ($P > 0.05$), tangent modulus of the distilled water group was statistically smaller than all of other groups ($p > 0.05$). Relaxation percentage for dehydrated specimen was less, as shown in Figure 4.9. Generally, the collagen fibrils stay in the minimum potential energy state and after applying load, they re-orient and move to regain minimum possible potential energy state. In the specimen with expanded matrix, the higher degree of freedom and more space for relative movement, as shown in Figure 4.10, let the collagen fibrils to orient better in direction of applied force; thus, higher portion of applied load was dropped

and the specimen relaxed more. It has been reported that hydrated tendon and ligament relaxed faster and more in stress relaxation test[68-71].

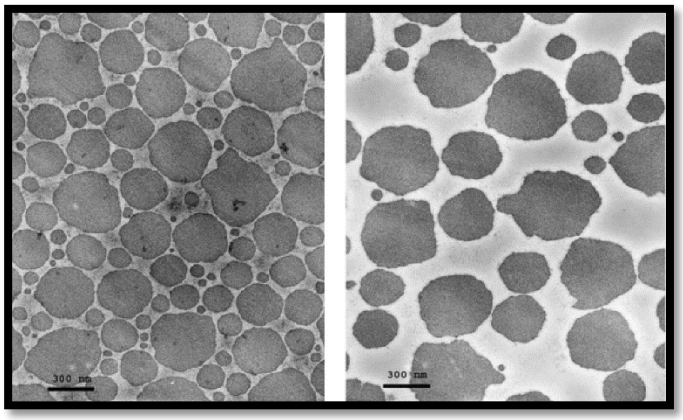

Figure 4.10. TEM images of transverse section of tendon showing fibrils in (left) normal, and (right) PBS-incubated samples (with permission from[72]).

The experiments show that as the cornea becomes hydrated, the stiffness decreases. In water, the extracellular matrix of stroma expanded greatly, and it can be assumed that only collagen fibrils are responsible for load bearing of stroma. According to this assumption, a model was proposed to show the effect of matrix mechanics on the less hydrated groups. The formulation for this model is as follows,

$$\sigma = \sigma^C + \sigma^M \tag{10}$$

$$\sigma^C = A(e^{B\epsilon} - 1) \tag{11}$$

$$\sigma^M = C\epsilon^2 \frac{< t_w - t >}{< t_w - t >} \tag{12}$$

where σ^C and σ^M representing stress in the collagen fibrils and extracellular matrix, respectively. A, B, and C are parameters to be found from curve fitting. Thickness in water and any solution is denoted with t_w and t, respectively and < > represent so-called

Macaulay brackets. First, stress strain behavior of corneal stroma in water which was swollen, curve-fitted using Eq. *(11)*. Eq. *(10)* was applied to the other stress response data and C was calculated for each category using obtained A and B parameters for DI-water.

Curve fitting to the bathing fluid results based on the proposed model in Eqs. *(10)-(12)* are presented in Figure 4.11 and Table 4.2. The calculated parameters show that C parameter is increasing, with decrease in thickness. As the thickness (or hydration) decreases, the spring constant, C, increases, exponentially, i.e. $C = 990.4e^{-2.54\,t}$ as shown in Figure 4. 12; therefore, Extracellular matrix becomes stiffer and its mechanical properties becomes significant. This indicates that as hydration decreases, the role of proteoglycan and interfibrillar connections becomes more apparent in the mechanics of cornea[61, 73]. The proteoglycans may limit the relative sliding of fibrils and improve integrity of ultrastructure.

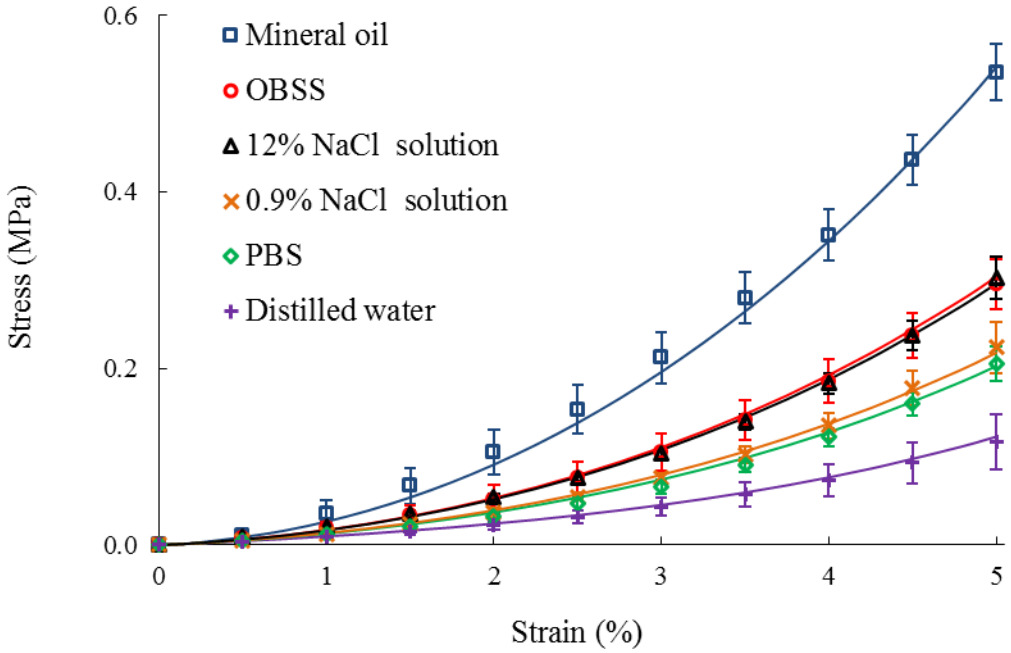

Figure 4.11. Stress strain behavior of corneal stroma in different bathing fluids and fitting lines obtained using proposed model

Table 4.2. Average calculated fitting parameters using suggested model in Eqs. (10)-(12)

Bathing Solutions	A (KPa)	B	C (MPa)
DI-Water	20.7	38.8	0
PBS			32.4
0.9% NaCl			35.4
12% NaCl			69.3
OBSS			72.4
Mineral Oil			167.6

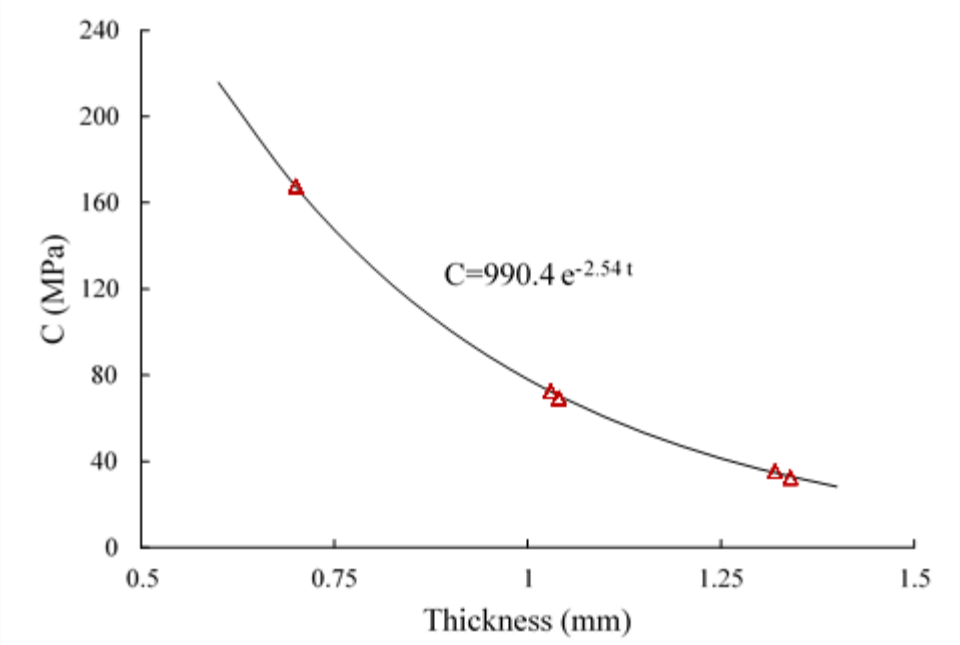

Figure 4. 12. Spring constant (C) and thickness plotted for all groups and an exponential line is fitted to the results, $C = 990.4e^{-2.54\,t}$.

4.3. Relation between thickness and mechanical behavior

In order to use the result of uniaxial tensile tests as a characteristic property of tissue, special care should be taken about sample conditions during experiments. Previous studies

have been done to characterize tensile behavior of cornea. Boyce et al[27] used bovine corneas with 1.15-1.30 mm thickness in uniaxial tensile test. In the Holtzel et al's study[49], tensile test was done on bovine strips with 1.53 mm thickness[49]; however, the physiological thickness of bovine cornea is 0.75-0.87 mm[74]. In the previous studies, there are inconsistency in the specimen's thicknesses that were used during the tensile test.

To examine the effect of thickness on mechanical properties, tensile tests were done on strips with different thicknesses and the force relaxation was collected for 2000s. Captured images showed that the thickness change in oil is negligible. Stress response in tension and relaxation for thickness groups are presented in Figure 4.13(a) and (b), respectively. The results depicted that with increasing thickness, extensibility of cornea increases and stiffness decreases. Force strain responses are also presented in Figure 4.14. Tangent modulus, thickness, and hydration for every thickness group was calculated at 5 % strain in Figure 4.15. Tangent modulus for less hydrated samples is lower and the difference between all groups was statistically significant. Stress at 5% strain and equilibrium stress after 2000 seconds for different thickness categories are presented in Figure 4.16. The failure behavior of bovine cornea is presented in Figure 4.17. First failure point was at 28.7%±1.2% strain and 6248.6 KPa±984.2KPa. The final failure strain was 31.5%±1.3% and failure stress was 6373.7KPa±1656.1KPa.

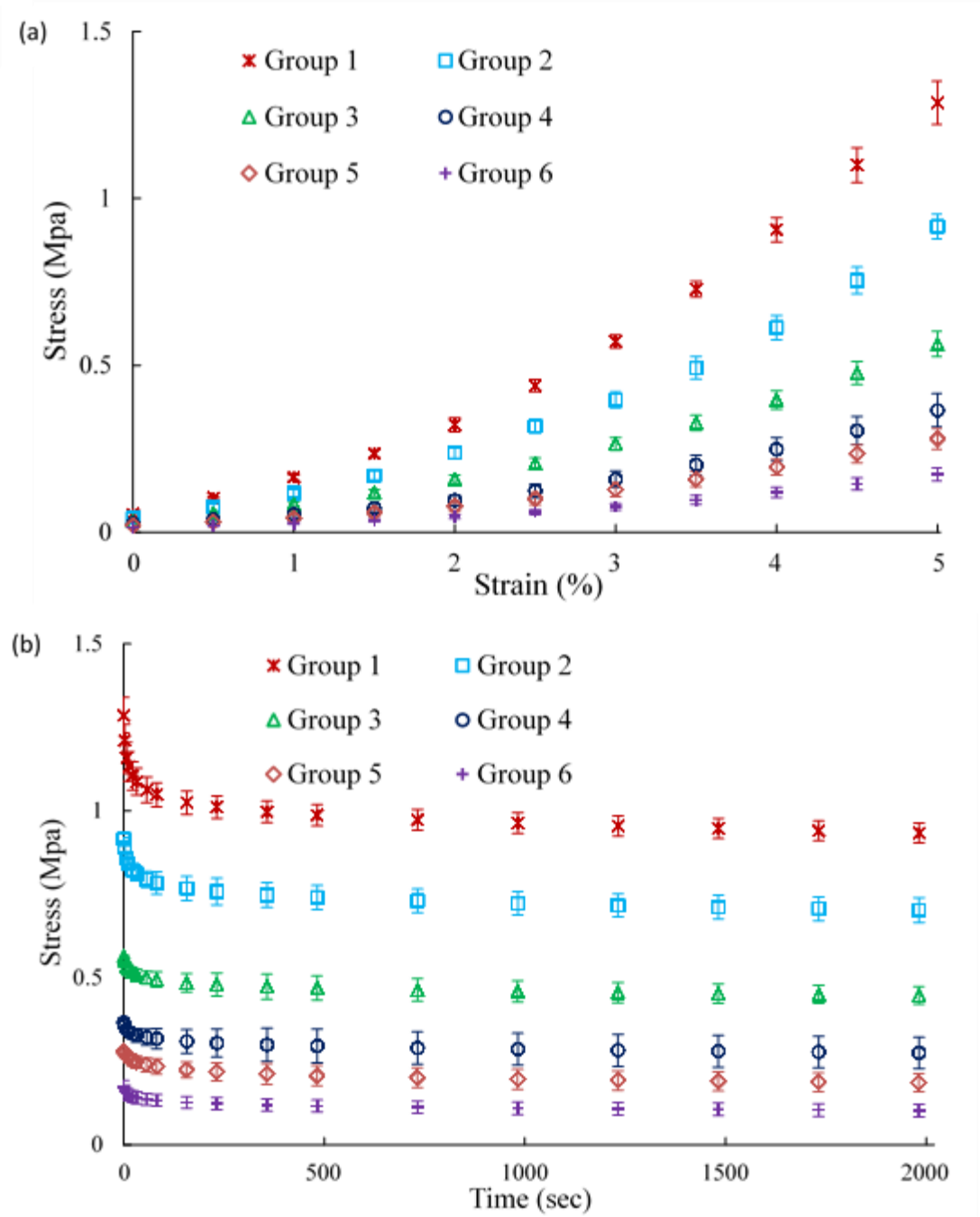

Figure 4.13. (a) Stress response in tension, (b) stress relaxation for thickness groups. Specimen with smaller thickness show stiffer behavior.

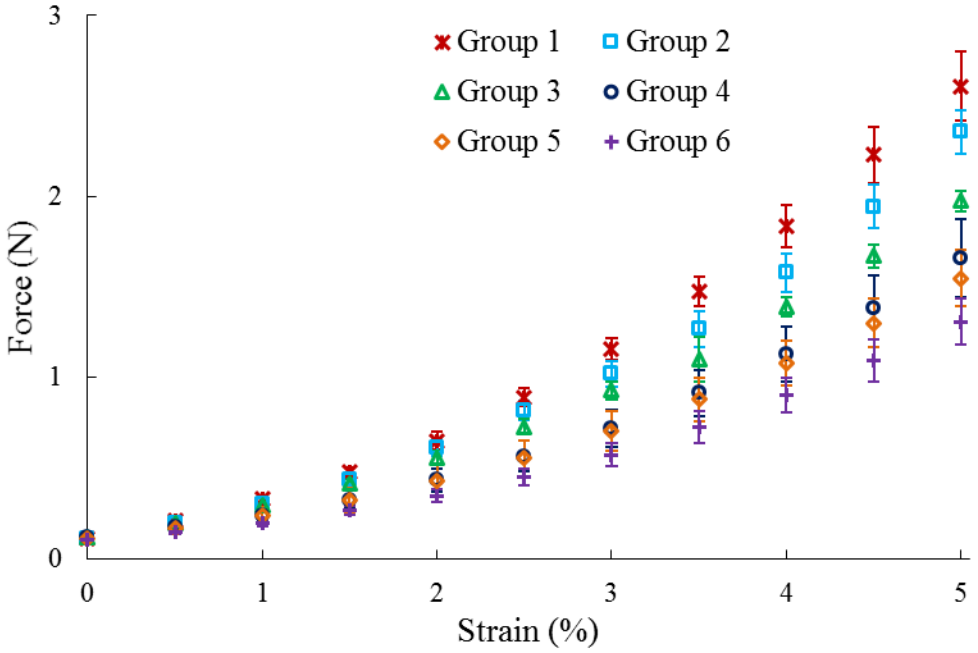

Figure 4.14. Force strain behavior of thickness groups.

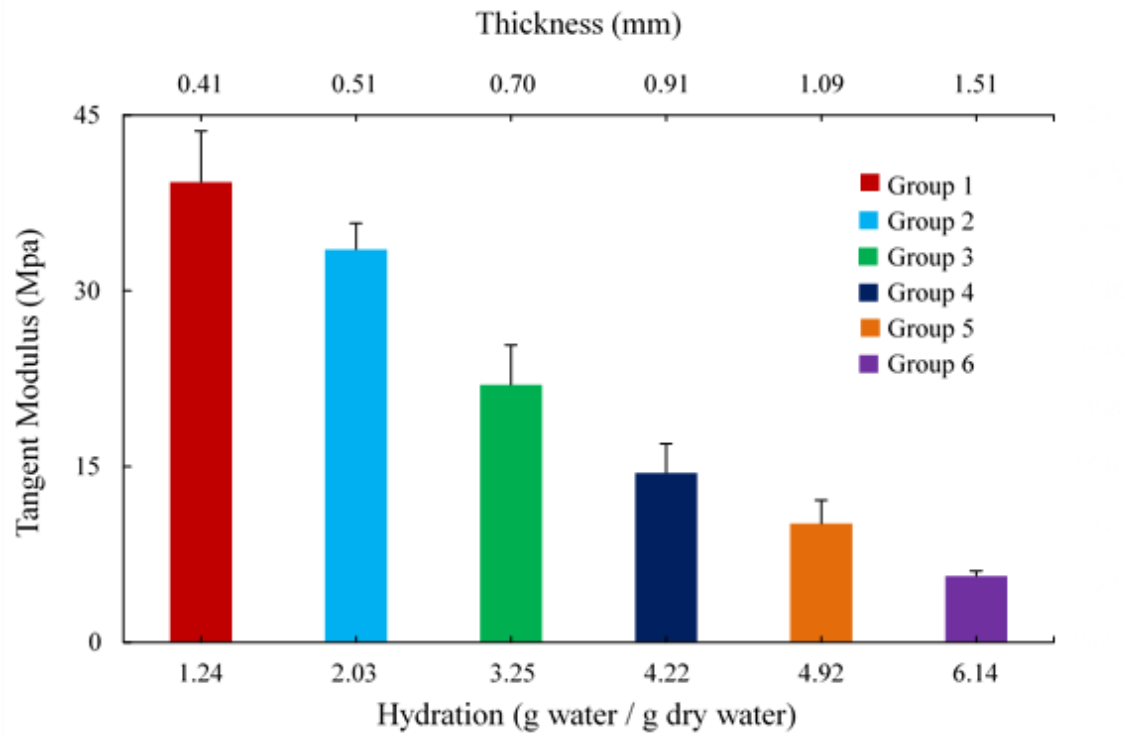

Figure 4.15. Tangent modulus, thickness, and hydration for every thickness group were calculated at 5 % strain

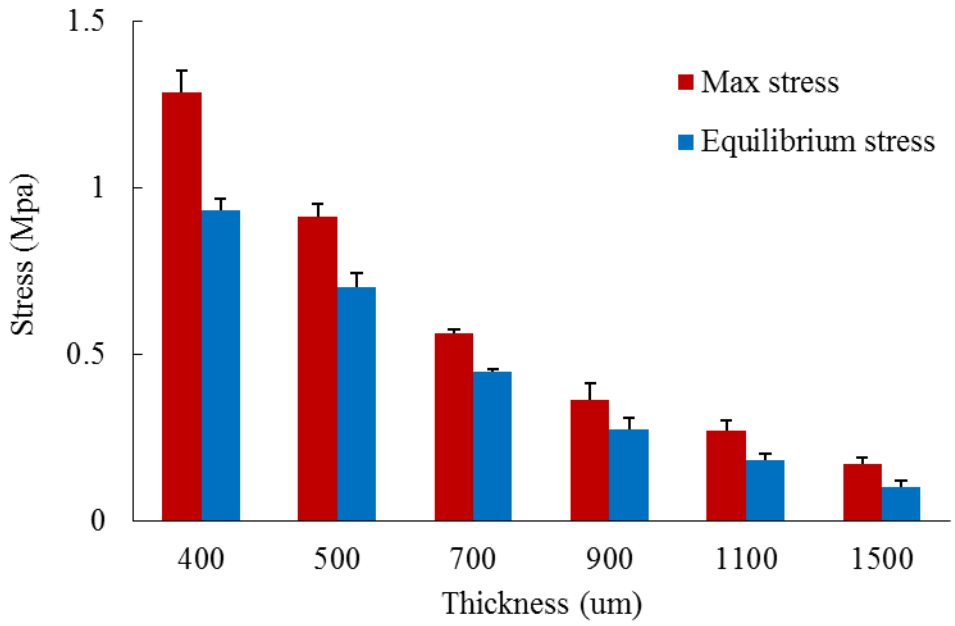

Figure 4.16. Average measured stress at 5% strain and equilibrium stress after 2000 seconds for different thickness groups.

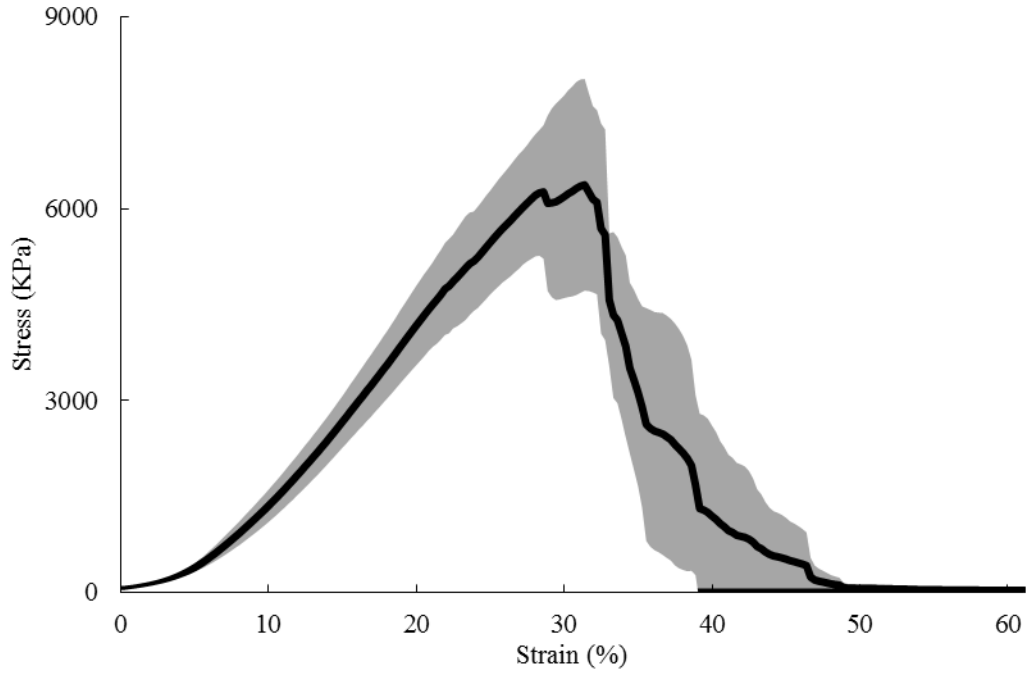

Figure 4.17. Average stress strain and failure point of bovine strips (Shaded area shows standard deviation). First failure point is at 28.7%±1.2% strain and 6248.6 KPa±984.2KPa. The final failure strain was 31.5%±1.3% and failure stress was 6373.7KPa±1656.1KPa.

The viscoelastic response of specimens in six thickness groups in mineral oil was analyzed. The results further supported our earlier work on hydration dependent properties of cornea. By using mineral oil as a bathing solution, the hydration was kept constant; so, it becomes possible to investigate the effect of water content difference on biomechanical properties. Strips with higher cross section shows softer stress strain and relaxation behavior as shown in Figure 4.13. Forces for 400 µm and 500 µm at 5% strain were higher than forces for 1100 µm and 1500 µm, respectively.

Conducting experiments on the cornea with different thicknesses indicated that hydration and water content have a significant effect on the tensile properties. It has been reported that water content affects the corneal shape and radial distribution of strain and stress[1] and in the inflation test. Hjortdal[75] observed the hydrated cornea had less strength because of collagens relaxation in extracellular matrix. When cornea swells over physiological hydration, cornea loses transparency. Negative charges of GAGs attract the water molecule inside the cornea. Increased water content affects the matrix and collagen fiber organization; so the mechanical properties change.

This thesis did not study why the cornea has hydration-dependent properties; nevertheless, it is speculated that any change in collagen fiber density and matrix integrity directly affects tissue mechanics. As corneal thicknesses increases, the matrix expands and the distance between fibrils increases[12, 76, 77] as shown in Figure 4.18; therefore, some of covalent bonds between collagen fibrils and proteoglycans break. This change leads to more extensibility of the tissue. This reduces the strength against shear load between fibrils and they can slide easier relative to each other. Therefore, as the thickness (or water content) increases, the corneal stiffness reduces, Figure 4.15.

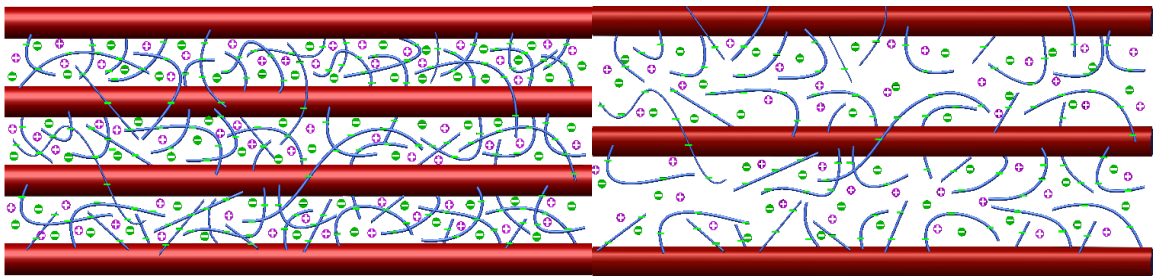

Figure 4.18. Fibrils and proteoglycans distribution in (left) normal cornea, (right) swollen cornea (horizontal cylinders and curve lines present fibrils and proteoglycans, respectively, and the positive and negative signs stand for charges in the cornea.

The result of uniaxial tensile test on the stroma with different thicknesses are used to curve fit using both exponential and power formulas. Figure 4.19 shows the experimental data and fitting lines using both formulas. The obtained value for A, B, α, and β are displayed in Table 4.3. Plotted figures and also goodness of fit (R^2) shows that these two formulas are appropriate to fit the experimental data.

Table 4.3 Average material parameters obtained from curve fitting to the results of uniaxial tensile test on the cornea with different thicknesses.

Thickness (mm)	$\sigma = A\varepsilon^B$			$\sigma = \alpha\left(e^{\varepsilon\beta} - 1\right)$		
	A (KPa) (10^3)	B	R^2(%)	α (KPa)	β	R^2(%)
0.5	129.2±24.3	1.67±0.07	99.7	245.5±25.4	31.1±2.2	99.7
0.7	72.6±13.3	1.64±0.06	99.5	155.4±33.2	30.3±3.5	99.6
0.9	55.2±10.9	1.70±0.08	99.6	94.9±9.1	30.4±2.2	99.6
1.1	40.6±3.2	1.69±0.06	99.3	72.9±14.7	30.5±2.9	99.6
1.5	28.9±2.7	1.74±0.03	99.8	43.6±7.3	30.5±2.2	99.6

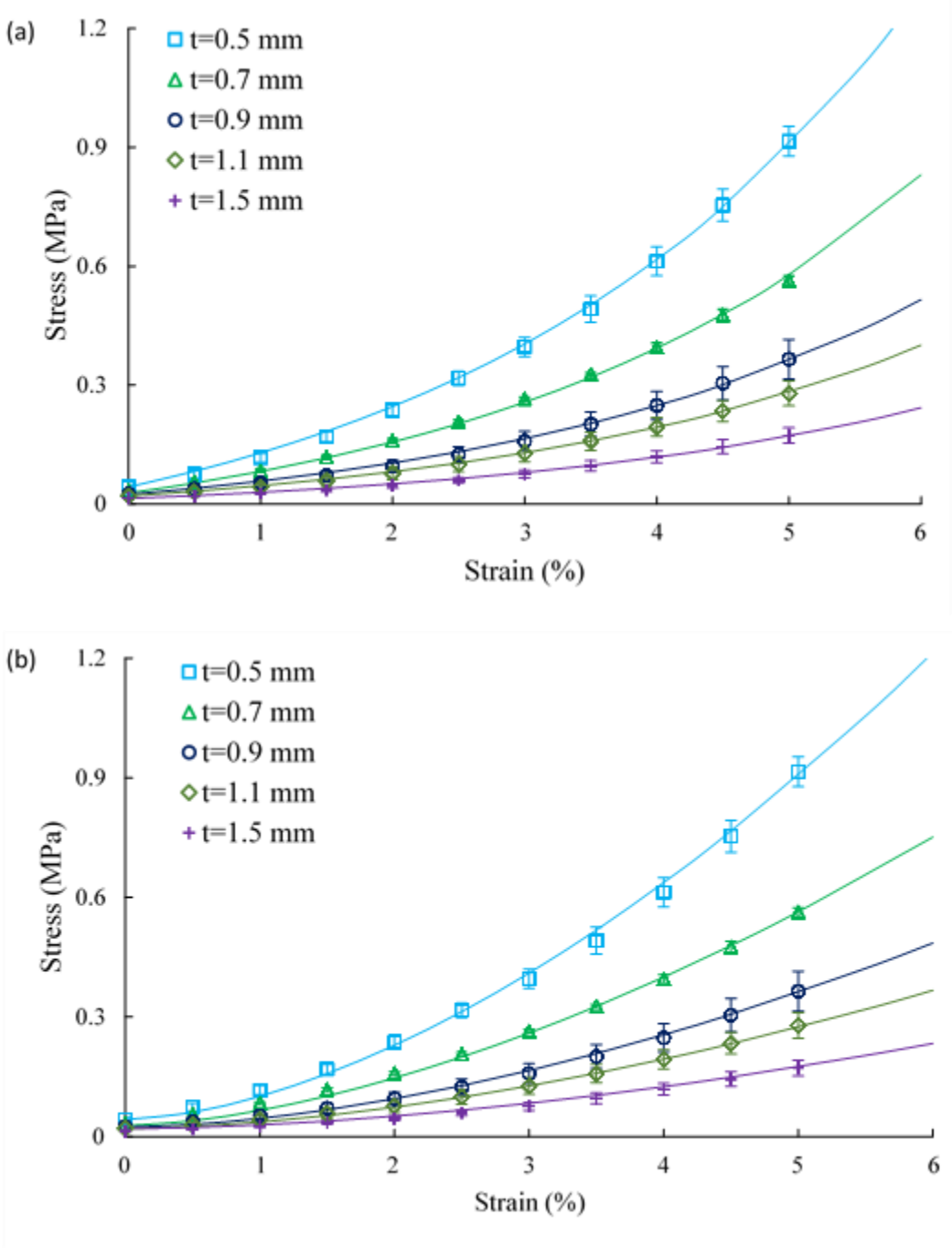

Figure 4.19. Stress strain behavior of stroma with different thicknesses: solid lines show the fitting lines using (a) exponential formula, and (b) power formula.

In both equations, A and α are a factor to show rigidity of stress response and B and β are showing non-linearity response of specimen. The fitting parameters listed in Table 4.3 indicated that non-linearity in the stress strain behavior of corneal stroma does not change

with thickness change. The maximum change in non-linearity were 2.3% and 3.6% for exponential and power law, respectively, which are not significant. The stress range changes greatly in different thickness groups and A and α changes accordingly. Average increase per each group starting from 1.5 mm to 0.5 mm are 52.5% and 56.6% for A and α, respectively. Generally, for the stiffer specimen, A and α increase while, the non-linearity parameter remains approximately constant. Since, the physiological corneal thickness is 0.75 mm-0.87 mm, the two thickness groups of 700 μm and 900 μm were chosen to present stress strain behavior and tangent modulus of cornea at physiological thickness in the in vitro condition.

4.4. Riboflavin/UVA Crosslinking Treatment

Uniaxial tensile test and following stress relaxation test were used as proper tools to examine biomechanical properties change after crosslinking treatment and how the corneal stiffness is changed. Most of previous studies have applied crosslinking treatment on the anterior side of cornea[35, 37, 46]. Average thickness of cornea, pre-treatment and post-treatment were 750±28 μm and 671±30 μm, respectively. A significant decreases in thickness was observed post treatment ($p > 0.05$). The thickness decrease post treatment has also been reported previously statistically significant[38, 43]. It is proposed that high concentration of dextran and its high molecular weight causes dehydration of cornea.

Pilot experiments were done to choose testing conditions, and initial and final thicknesses were measured. It is known that as tissue stretched to high strains, the fluid starts to move out of tissue[71], so the thickness will change. It was observed that specimens that were tested with initial thickness about 900 μm experienced minimum thickness change. In addition,

OBSS solution was used as bathing fluids which is a qualified ophthalmic solution and previously has been used for submersible mechanical testing on cornea[27].

4.4.1. Uniaxial tensile and stress relaxation test

Riboflavin/UVA crosslinking has been introduced as a new treatment for Keratoconus disease[35, 36, 46] which has many advantages over previous methods. In this process, there is no need for cutting a flap from cornea and recovery time after treatment is quick and painless. Previous works studied the effect of crosslinking on different properties of cornea like enzymatic digestion[78], possible damage to the corneal layers[36, 79], fiber diameter change[38, 80], hydration behavior[38, 81], stiffness[41, 82], corneal curvature[36, 83], and Keratocytes loss[39, 40, 84]. However, this study focused on mechanical properties change after crosslinking treatment. Uniaxial tensile test along with dynamic test provides enough data to analyze viscoelastic behavior change of cornea and understanding of how microstructure change affects the biomechanical response of tissue. In addition, the effect of thickness and hydration on biomechanical response of crosslinked cornea under tension was characterized.

Uniaxial tensile test showed significant change in the biomechanical properties of cornea. Figure 4.20 implies that the crosslinking treatment stiffened the cornea. Average peak stress of Crosslinked group was significantly higher than peak stress of control groups. The peak stress increased 79.5% for Crosslinked group comparing to control group. Figure 4.21 shows stress relaxation response of specimen to the constant strain. At the first 100 seconds, stress dropped quickly and after that stress slope decreased with lower slopes continuously.

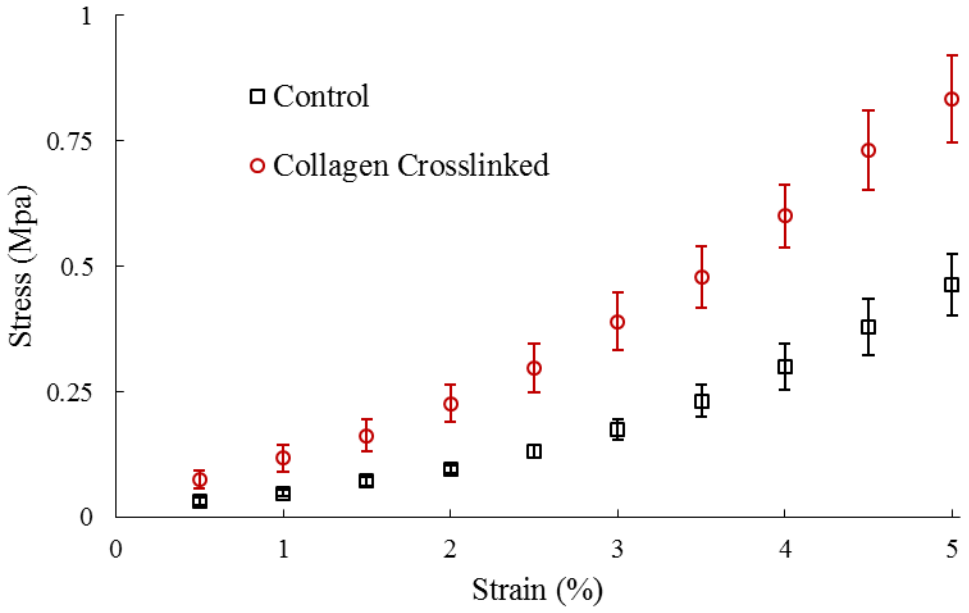

Figure 4.20. Average stress strain behavior of control and collagen crosslinked group. The curves show clear increase in the stress response of crosslinked cornea.

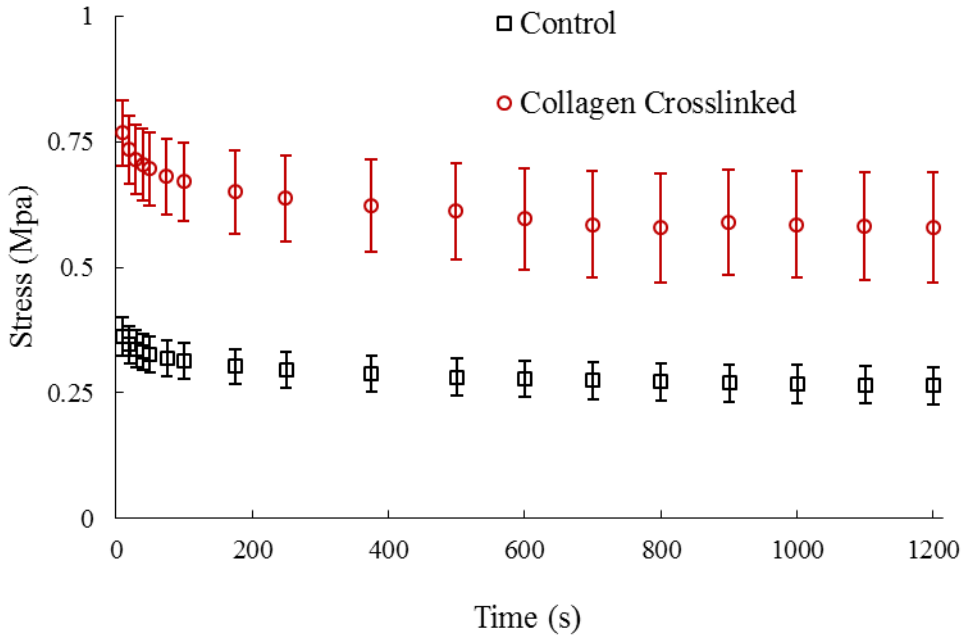

Figure 4.21. Stress relaxation behavior of corneas after applying 5% strain.

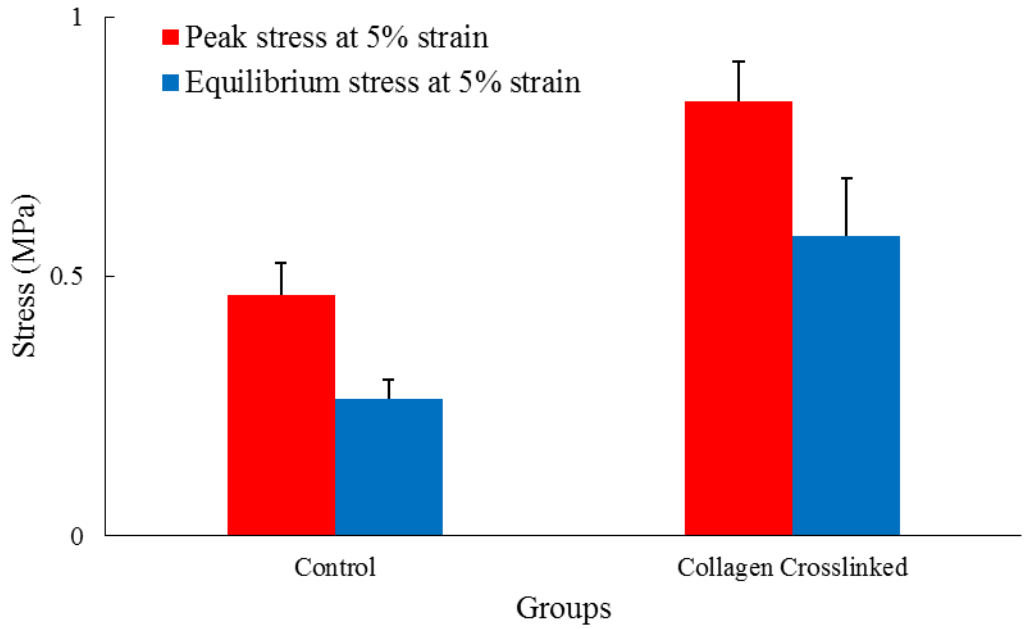

Figure 4.22. Peak and equilibrium stress at 5% strain of collagen crosslinked and control groups.

Peak and equilibrium stresses at 5% strain are shown in Figure 4.22. Collagen crosslinked group has significantly higher peak and equilibrium stresses compare to the control group ($P > 0.05$). Relaxation percentage for the control group (43.1±2.4 %) is higher than crosslinked group (31.4±8.7 %) and as the sample becomes stiffer, the relaxation percentage reduces.

The mechanical testing showed that crosslinking treatment increased stiffness of cornea. Wollensak et al[41] reported 328.9% and 71.9% increase in uniaxial stress for human and porcine cornea, respectively. The difference between stress strain behavior of our result with Wollensak et al[41] can have several reasons. In addition to species difference, preconditioning has a considerable effect on the biomechanical response of soft tissues. In the current study, preconditioning was used, while Wollensak et al[41] did not apply preconditioning. It has been shown that the cornea is a strain rate dependent[48, 67, 85] and

using higher displacement rate in the current study (5 mm/min) than Wollensak et al[41] (1.5 mm/min) results in the higher stress strain behavior.

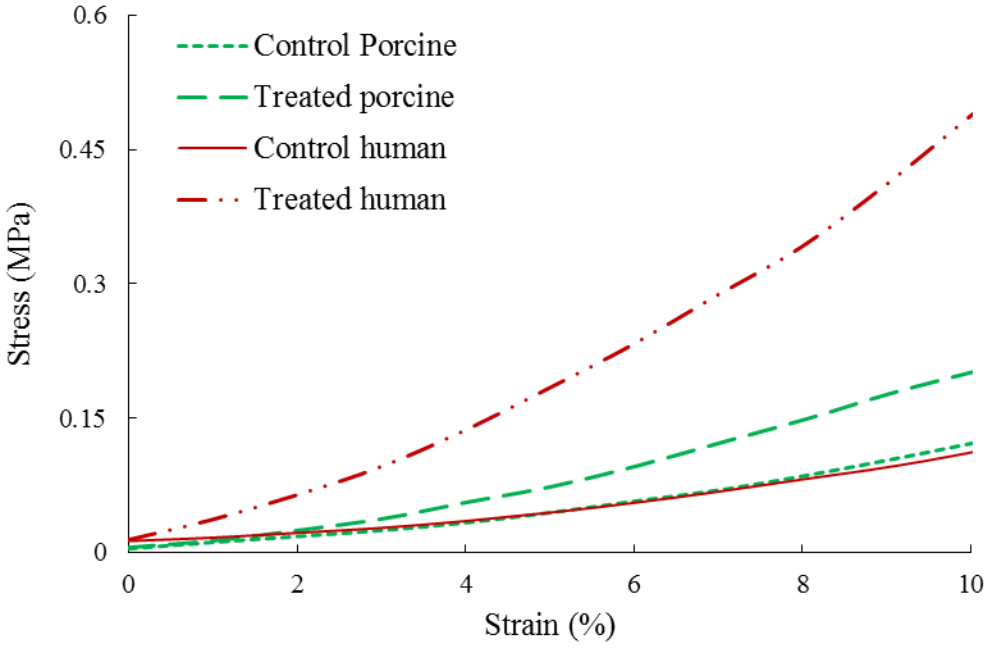

Figure 4. 23. Stress strain behavior of control and treated porcine cornea. (the data is taken from[41])

It has been believed that interfibrillar bonds are less possible to form in process of crosslinking[38, 41, 45] and new bonds are created in the intrafibrillar space. New connections between and within collagen molecules, between and within proteoglycans, and between proteoglycan and collagen molecule are mentioned as newly formed crosslinks[38, 86].

It has been found that in the linear region of stress strain behavior, over 60% of deformation happens because of sliding fibrils relative to each other[87]. Since, proteoglycans are the links between collagen fibrils[88], the new bonds limit the fibrils to slide freely relative to each other. The new formed links between and within proteoglycans have been accounted for

increased stiffness of cornea[86]. It has also been reported that shear resistance of cornea improves after crosslinking[42].

These newly formed bonds may enhance the integrity of fibrils and make them stronger under tension load. It is obvious that in the crosslinked cornea with new links formed around fibrils, their movement is limited and fibrils cannot change the orientation easily. The result is that stress (or force) reduces in the crosslinked cornea.

Stress strain behavior of collagen crosslinked corneas with different thicknesses are presented in Figure 4.24. Stresses at 5% strain were increased for all of thickness groups comparing to control groups. Figure 4.25 shows the stress relaxation response of the collagen crosslinked groups. Figure 4.26 compares the relaxation percentage of the control and collagen crosslinked groups. At lower thicknesses, the crosslinked group had significantly lower relaxation percentage, but the difference became smaller as the thickness increased. Tangent modulus of control and crosslinked groups at 5% strain for different thickness groups are shown in Figure 4.27. In all of thickness groups, tangent modulus of crosslinked groups significantly higher than control groups ($P > 0.05$).

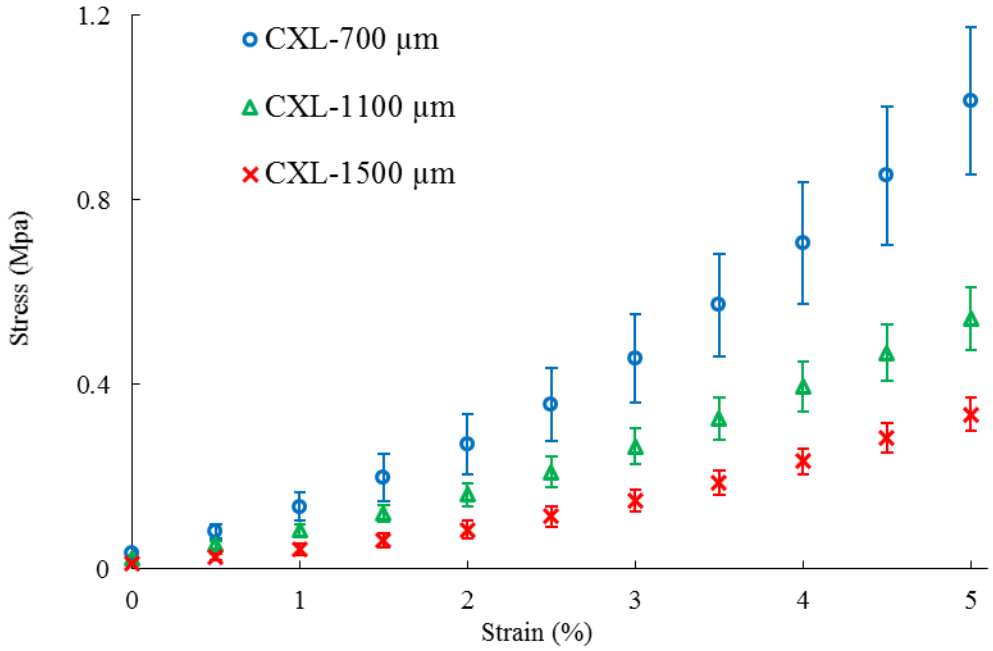

Figure 4.24. Stress strain behavior of collagen crosslinked with different thickness groups.

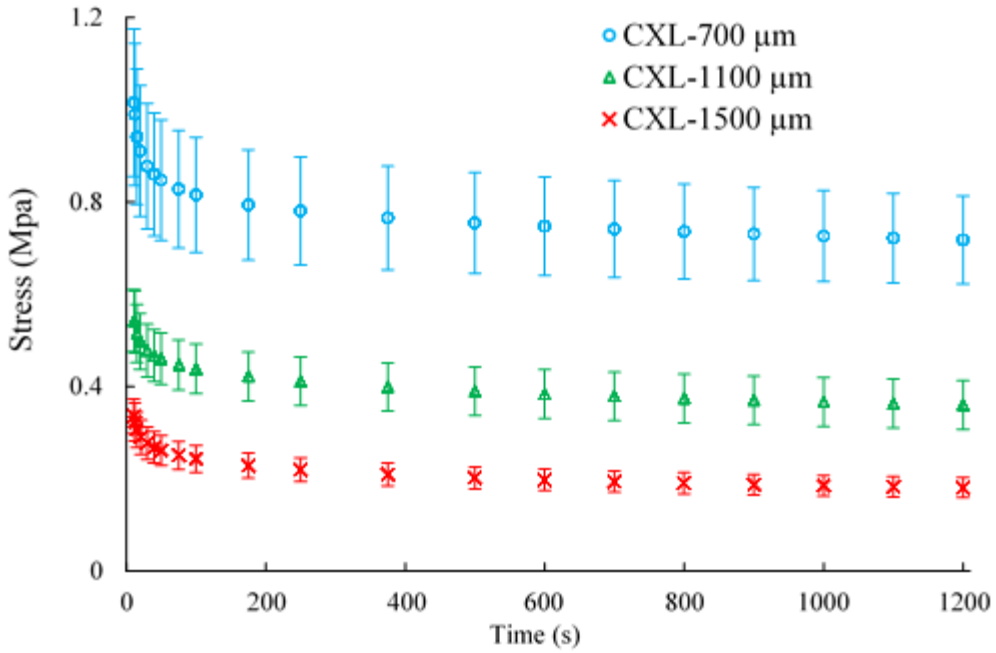

Figure 4.25.Stress relaxation behavior of collagen crosslinked thickness groups

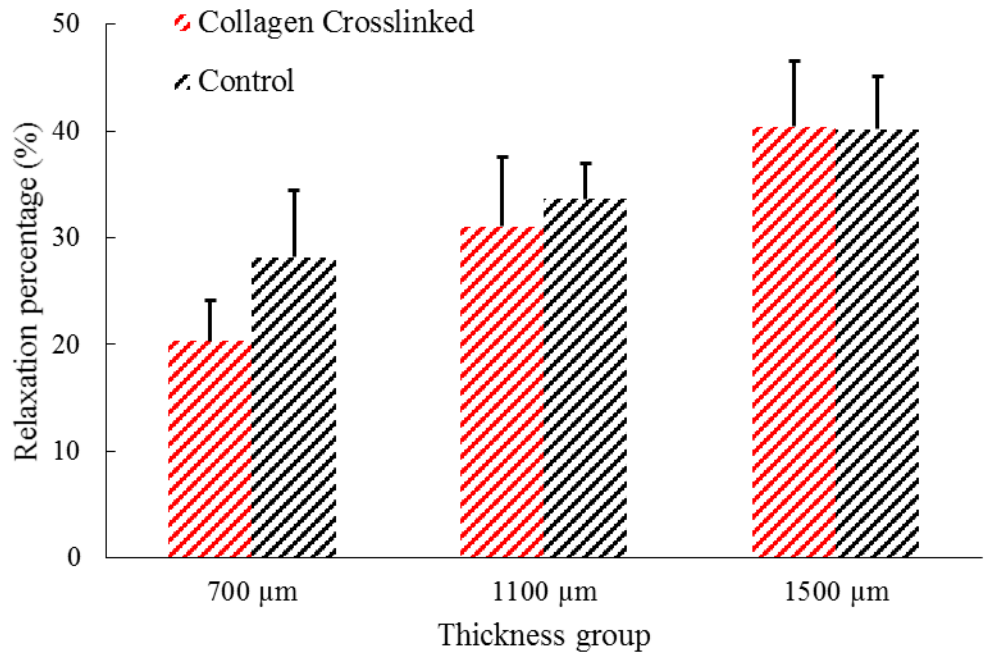

Figure 4.26. Relaxation percentage at 5% strain for control and collagen crosslinked groups at different thicknesses.

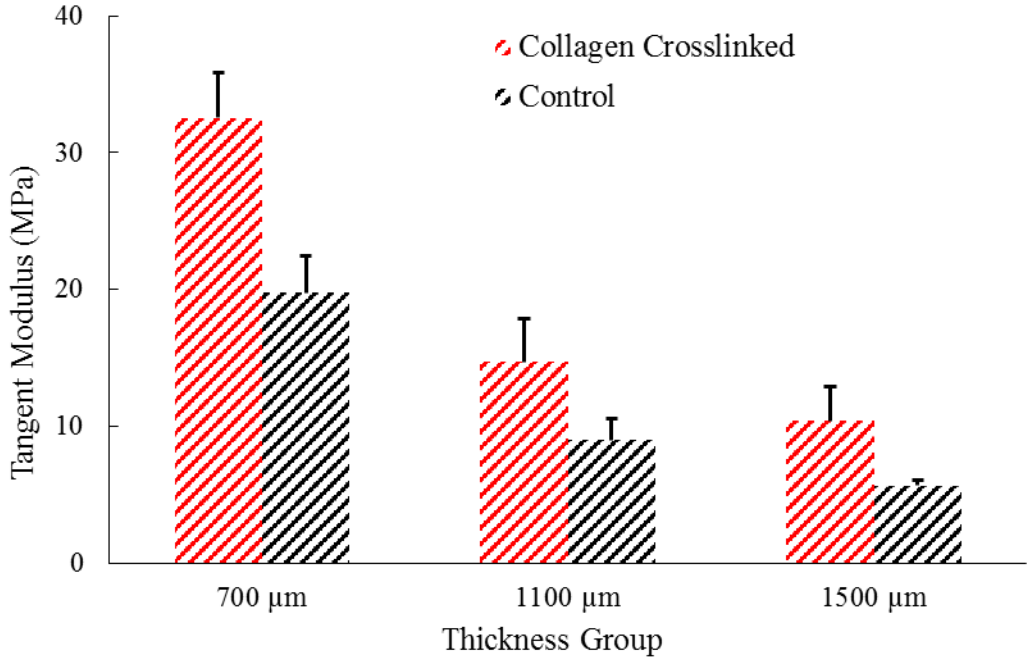

Figure 4.27. Tangent modulus of control and crosslinked groups at 5% strain for different thickness groups

Riboflavin/UVA crosslinking enhanced the biomechanical properties of bovine corneal stroma and stress significanly increased in the collagen crosslinked group. The reduced relaxation percentage for the crosslinked group might be an evidence that shows newly formed bonds in the crosslinked stroma do not let the collagen fibrils and proteoglycans slide and re-orient easily; so, the matrix and collagen fibrils integrity increases.

Previously, it has been reported that thickness (or hydration) significantly affects the mechanical properties of cornea[85, 89]. In this study, as the thickness increased, stress strain behavior became softer and the increase in the maximum applied stress decreased from 94.7% to 75.8% In addition, the observed difference in relaxation percentage reduced from 7.9% for 500 μm thickness group to approximately zero for 1500 μm thickness group. The observed trend shows that at higher thicknesses, the new bonds have less effect on the mechanics of cornea because of expanded matrix and higher interfibrillar spacing. Therefore, it can be concluded that hydration has an important effect on the collagen crosslinking treatment. Based on this conclusion, crosslinking treatment effect on biomechanical properties should be determined at specified hydrations.

4.4.2. Dynamic mechanical analysis

Few previous studies focused on dynamic properties of cornea and other parts of eye[29, 90, 91]. Studying dynamic behavior of eye and its parts is important because of dynamic loads are applying to the eye in the routine life, i.e. eye movement, blinking, eye rubbing, body position change, and intraocular pressure (IOP) pulse. At each heartbeat, due to pressure change in blood stream entering eye, IOP oscillates accordingly for a few mmHg[92], so this pressure change affects the stress and strain in cornea, sclera, optic nerve, and other parts

of eye. IOP pulse can be considered as a primary risk factor for glaucoma and damage to optic nerve[93].

Several viscoelastic parameters of material such as storage modulus, loss modulus, and tan(δ) may be measured in the frequency sweep test. Average storage modulus for frequency sweep test with 0.1% strain amplitude for control and collagen crosslinked groups at 5% strain are presented in Figure 4.28. Crosslinked cornea had higher storage modulus than the control cornea. Loss tensile modulus decreased from 0.01 Hz up to 1 Hz and after that starts to increases up to 20 Hz for all groups at 5% strain, see Figure 4.29. Like storage modulus, crosslinked group had higher loss moduli. The tan(δ) behavior can be predicted based on the storage modulus and loss modulus behavior as shown in Figure 4.30

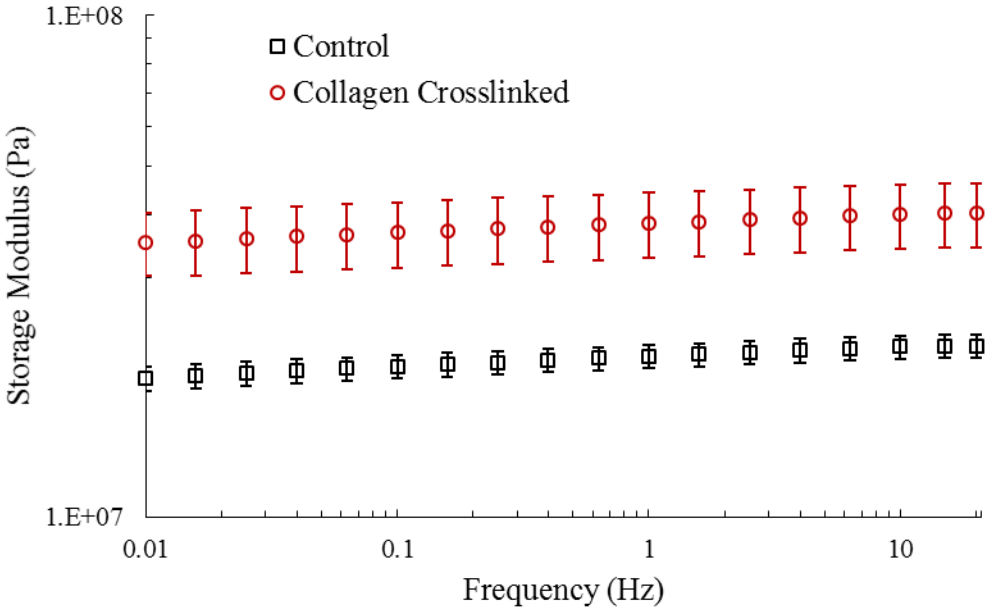

Figure 4.28. Average storage modulus for frequency sweep test with 0.1% strain amplitude for control and collagen crosslinked groups at 5% strain.

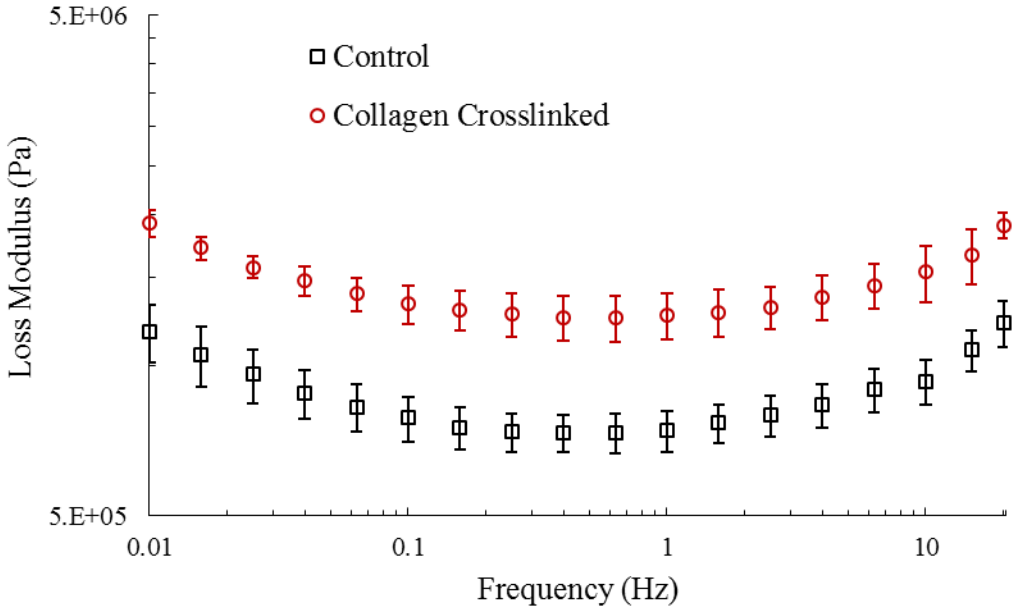

Figure 4.29. Measured loss modulus behavior with frequency change at 5% strain.

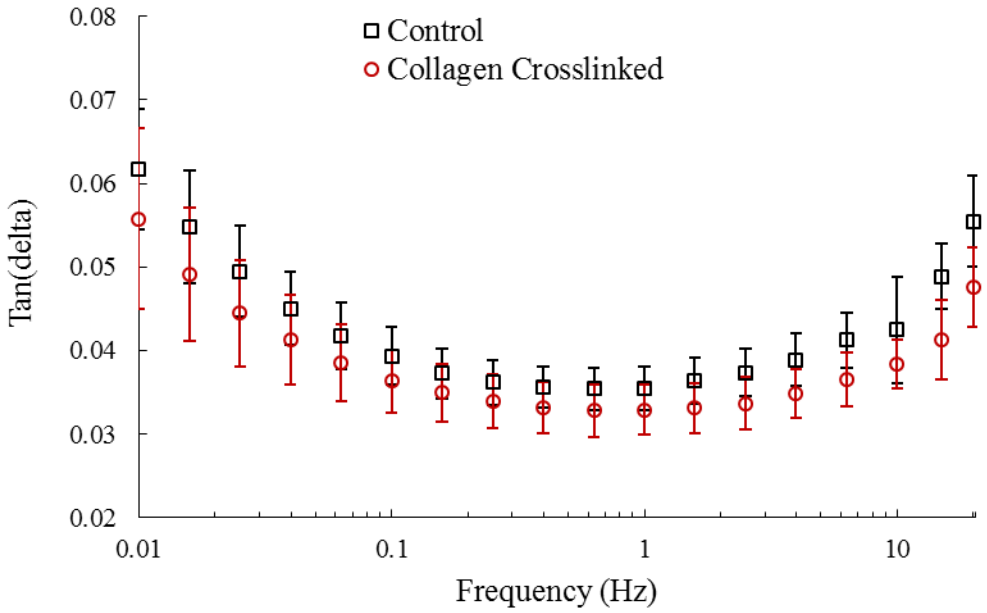

Figure 4.30. tan(δ) change in frequency sweep for all groups at 5% strain. The loss tangent modulus from frequency of 0.01 Hz to 1 Hz decreases and after that up to 20 Hz, increases slightly.

At high frequencies, data collecting may include device error and noise, so the accuracy of device plays a major role in collecting trustworthy data. The device (RSA-G2, TA instrument, Delaware, USA) was used here is one of the most advanced mechanical analysis platforms which is designed for conducting various experiments in very low to high displacement rates and in a wide range of frequencies from 2 μHz to 100 Hz. Frequency higher than 20 Hz was not used in the current study to prevent any noise in data. The separate motor and transducer system ensures precise measurement of displacement and force independently. In addition, testing cornea in the bathing fluid was feasible by the submersible chamber.

As the frequency increases, storage modulus increases which shows that when the load applies with high speed, the tissue acts more like a spring. The same behavior was observed for other connective tissues[29, 91, 94-97]. Average measured storage modulus for control cornea (18.9-21.9 MPa) was consistent with the previous reported data for cornea by Kaplan and Bettelheim[29]. In their study, the storage modulus at frequency range of 3.5 to 110 Hz was equal to ~8-20 MPa. There could be different reason for observed slight difference in the results of this study and previously reported data. The first reason could be preconditioning procedure that was used in our study. In addition, the steady state strain is not same and also the thickness (or hydration) is not mentioned for Kaplan and Bettelheim studies. The average storage modulus for tendon and ligament was measured in the approximate range of 4 to 1800 MPa[95, 98], which our result are in this range however, tendon is generally stiffer than cornea.

The average loss modulus for control cornea (1.17-1.22 MPa) was in the comparable range with loss modulus of other connective tissues[29, 95]. Previously, in a temperature sweep dynamic test on cornea, average loss tensile modulus was reported from 0.2 to 1.0 MPa[29]. The average tan(δ) in both groups were measured from 0.035 to 0.060, which shows that cornea is more like an elastic material than a viscous material. The cornea's damping value was obtained as 0.05 to 0.07 for frequencies in the range of 3.5 Hz to 110 Hz[29], which is consistent with our data for control group (from 0.055 to 0.062). From 1 Hz to 20 Hz, damping ratio increased and the same trend was observed for cornea in frequencies increasing from 3.5 Hz to 110 Hz[29]. The tan(δ) for ligament and lung was reported ranging 0.01-0.02 and 0.06-0.13, respectively[99]. Canine sclera have been shown to have tan(δ) values in the range of 0.101-0.134[93]. The measured tan(δ) for cornea in the current study is in the good agreement with reported value for other soft tissues.

The observed trend for tan(δ) (decreases from 0.01 to 1 Hz and increases afterwards) is similar to the trend has. Decrease of tan(δ) for crosslinked groups showed that ratio of mechanical energy storage to energy loss increases after crosslinking. Elevated elastic behavior could be because of interactions between proteoglycans and collagen fibrils. More bonds between proteoglycans, collagen molecules, and fibrils in the crosslinked cornea at higher tension make the structure more solid and increases the ability to better store mechanical energy in the dynamic loading[93].

The lower damping ratio may have some side effects on stress distribution on other parts of eye such as sclera. Crosslinking treatment effect on relative collagen fiber sliding and possible friction between matrix and collagen fibers were considered as potential reasons

to affect dynamic properties[100, 101]. This observation is consistent with previous reports which has been shown that crosslinking within fibrils has a major role in resisting dynamic deformation in sclera [97]; It has also been observed that these connections have a significant effect on the stiffness of aortic tissue [102] and tendon [103].

4.5. Limitation

There are some drawbacks in performing steady state uniaxial tensile and dynamic experiments in the in-vitro condition. In the sample preparation process, the sample was cut using a custom built two bladed part; however, special care was taken to have the exact and straight cut.

Straightening the initial curvature of cornea produces compression forces on the both anterior and posterior side of specimen which is a necessary step in the beginning of uniaxial tensile step. Another drawbacks is assuming constant thickness in the whole length of cornea which is not true. Corneal thickness is minimum in the center and increases as moving from center to the limbus, but the change is hard to measure during experiment. Also, uniaxial tensile test is applying load in just one direction while the cornea is under pressure multi-axially in all directions.

Chapter 5

Conclusions and Future Work

5.1. Conclusions

Biomechanical properties of bovine corneal stroma was studied in the uniaxial tensile test. Strain rate dependency and anisotropic properties of bovine cornea were investigated using uniaxial tensile test. Measured responses under different displacement rates showed that the cornea is strain rate dependent and it behaves stiffer under higher displacement rates. In addition, anisotropy of cornea was investigated by testing the strips cut in the IS and NT directions. The results showed that bovine cornea in the IS direction is stiffer than NT direction.

Bathing fluid effect on the mechanical properties of cornea was examined. Swelling behavior of cornea is not same in different bathing fluids, so the stress strain behavior will not be the same, accordingly. In addition, using proposed model to curve fit the experimental data, contribution of collagen fibrils and extracellular matrix was estimated. The conclusion was that as the cornea swells, the mechanical response from matrix becomes smaller and the connection between fibrils and proteoglycans in the less hydrated cornea can be modeled as a nonlinear spring.

The effect of thickness and hydration on the stress strain behavior and time dependent relaxation behavior was investigated. As the thickness increases, load bearing capacity decreases and specimen relaxes more. Stiffness of corneal stroma decreases significantly with increasing thickness or hydration.

Knowing the mechanical effect of Riboflavin/UVA crosslinking treatment, as a new treatment for Keratoconus disease, on the cornea has a great importance. Uniaxial tensile test showed significant increase in the stiffness of cornea post-treatment. In addition, it was observed that the crosslinking treatment improved the dynamic properties like storage modulus and tan(δ). Testing treated cornea with different thicknesses showed that hydration has an important effect on the measured mechanical properties; therefore, the crosslinking treatment effect should be reported at the specified thickness and hydration.

5.2. Future studies

Knowing the mechanics of cornea provides the ability to predict its behavior under different loading conditions. In order to have a better understanding of tissue mechanics, both modeling and experimental studies are essential. Previous studies used different constitutive modelings to predict biomechanical behavior of cornea[48, 104, 105]. One deficiency of most of previous studies was that they did not consider the effect of bathing fluids and swelling. In this thesis, the experimental results show that the bathing fluids and swelling of cornea affect mechanical behavior in the uniaxial tensile test. To consider bathing fluid effect, a biphasic model was used to assess mechanical properties of cornea. This work is a continuation of a previous work by Hatami-Marbini and Etebu[73], which was done to model the unconfined compression test on the cornea in our research group.

FEBio software (www.FEBio.org) was used to simulate the experimental conditions and find the exact mechanical properties. FEBio software is a finite element tool for analysis of problems in biomechanics.

Preliminary finite element analyses were done to find the permeability and elastic modulus. Figure 5.1 presents stress time response of both the theoretical and experimental results for bathing fluid groups. Theoretical fittings show that isotropic biphasic model is a good model to predict the corneal stroma behavior. The preliminary results were satisfactory and good fits were achieved. For the future work, this model will be developed to add the anisotropic and strain rate dependency properties of cornea.

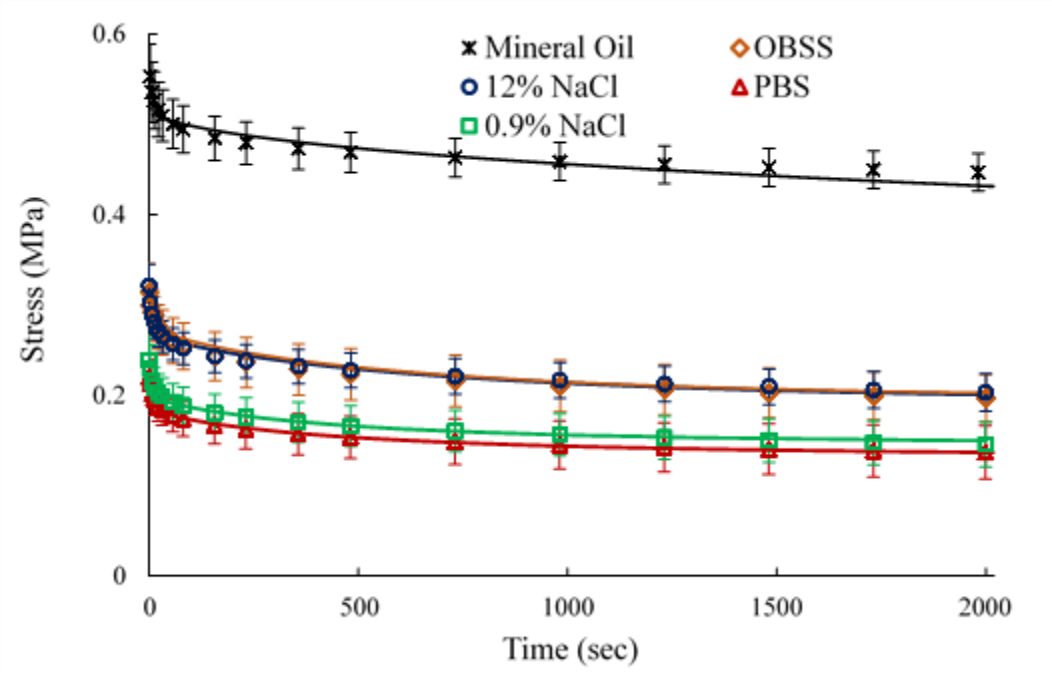

Figure 5.1. Stress time response of obtained from both modelling and experiments for bathing fluids groups.

To examine the effect of crosslinking treatment more precisely and localize the microstructure change, mechanical properties of corneal flaps should be studied. Preliminary uniaxial tensile test on the posterior and anterior flaps showed that stiffness increase in the anterior corneal flap is significantly higher. For the future, more tests are needed to be done to characterize steady state and time dependent responses of corneal flaps. In addition, taking TEM images may provide useful information on the difference of new formed bonds in the anterior and posterior flaps.

The dynamic tensile properties of normal and crosslinked cornea were determined in this thesis. To have a better understanding of needed improvement in the crosslinking treatment, it is essential to measure changes in mechanical properties due to the Keratoconus disease. For the future work, assessing dynamic properties of Keratoconus eyes is needed in order to provide beneficial data for judging the crosslinking treatment.

Most of previous studies have applied crosslinking treatment on the anterior side of cornea[35, 37, 46], however, there are some studies like Hayes et al[38] which performed crosslinking treatment on the posterior side of cornea. Our preliminary results showed that change in properties after treatment highly depended on the side of cornea that received the treatment. Further studies needs to be done in order to assess the effect of applying treatment on the anterior and posterior side of cornea.

References

1. Fratzl P. Collagen: structure and mechanics: Springer New York:; 2008.

2. Comaish IF, Lawless MA. Progressive post-LASIK keratectasia: biomechanical instability or chronic disease process? Journal of Cataract & Refractive Surgery 2002; 28:2206-2213.

3. Gray H. Anatomy of the human body: Lea & Febiger; 1918.

4. Valtot F, Kopel J, Haut J. Treatment of glaucoma with high intensity focused ultrasound. International ophthalmology 1989; 13:167-170.

5. Tan DT, Por Y-M. Current treatment options for corneal ectasia. Current opinion in ophthalmology 2007; 18:279-283.

6. Kamburoglu G, Ertan A. Intacs implantation with sequential collagen cross-linking treatment in postoperative LASIK ectasia. Journal of Refractive Surgery 2008; 24:S726.

7. Ehlers N, Hjortdal J. The cornea: epithelium and stroma. Advances in organ biology 2005; 10:83-111.

8. HANNA C, BICKNELL DS, O'BRIEN JE. Cell turnover in the adult human eye. Archives of ophthalmology 1961; 65:695-698.

9. Fratzl P. Collagen: structure and mechanics: Springer; 2008.

10. Beuerman RW, Pedroza L. Ultrastructure of the human cornea. Microscopy research and technique 1996; 33:320-335.

11. Daxer A, Fratzl P. Collagen fibril orientation in the human corneal stroma and its implication in keratoconus. Investigative Ophthalmology and Visual Science 1997; 38:121-129.

12. Meek KM, Leonard DW. Ultrastructure of the corneal stroma: a comparative study. Biophysical journal 1993; 64:273-280.

13. DRUBAIX I, LEGEAIS J, MALEK-CHEHIRE N, et al. Collagen synthesized in fluorocarbon polymer implant in the rabbit cornea. Experimental eye research 1996; 62:367-376.

14. Meek K, Fullwood NJ. Corneal and scleral collagens—a microscopist's perspective. Micron 2001; 32:261-272.

15. Scott JE, Haigh M. Identification of specific binding sites for keratan sulphate proteoglycans and chondroitin-dermatan sulphate proteoglycans on collagen fibrils in cornea by the use of cupromeronic blue in'critical-electrolyte-concentration'techniques. Biochem j 1988; 253:607-610.

16. Hayes S, Boote C, Lewis J, et al. Comparative study of fibrillar collagen arrangement in the corneas of primates and other mammals. The Anatomical Record: Advances in Integrative Anatomy and Evolutionary Biology 2007; 290:1542-1550.

17. Elsheikh A, Brown M, Alhasso D, Rama P, Campanelli M, Garway-Heath D. Experimental assessment of corneal anisotropy. Journal of refractive surgery (Thorofare, NJ: 1995) 2008; 24:178.

18. Meek KM, Boote C. The organization of collagen in the corneal stroma. Experimental eye research 2004; 78:503-512.

19. Boyce BL, Grazier JM, Jones RE, Nguyen TD. Full-field deformation of bovine cornea under constrained inflation conditions. Biomaterials 2008; 29:3896-3904.

20. Elsheikh A, Anderson K. Comparative study of corneal strip extensometry and inflation tests. Journal of the Royal Society Interface 2005; 2:177-185.

21. Woo SLY. Structural Analysis of a Corneo-scleral Shell: University of Washington.; 1971.

22. Triacca V, Spinelli L, Pandolfi A. Mechanical Characterization of Porcine Corneas.

23. Armstrong C, Lai W, Mow V. An analysis of the unconfined compression of articular cartilage. Journal of biomechanical engineering 1984; 106:165-173.

24. Ateshian G, Warden W, Kim J, Grelsamer R, Mow V. Finite deformation biphasic material properties of bovine articular cartilage from confined compression experiments. Journal of biomechanics 1997; 30:1157-1164.

25. Hatami-Marbini H, Etebu E. Hydration dependent biomechanical properties of the corneal stroma. Experimental eye research 2013; 116:47-54.

26. DiSilvestro MR, Suh J-KF. A cross-validation of the biphasic poroviscoelastic model of articular cartilage in unconfined compression, indentation, and confined compression. Journal of biomechanics 2001; 34:519-525.

27. Boyce B, Jones R, Nguyen T, Grazier J. Stress-controlled viscoelastic tensile response of bovine cornea. Journal of biomechanics 2007; 40:2367-2376.

28. Kampmeier J, Radt B, Birngruber R, Brinkmann R. Thermal and biomechanical parameters of porcine cornea. Cornea 2000; 19:355-363.

29. Kaplan D, Bettelheim FA. Dynamic rheooptical behavior of isolated bovine cornea. Biophysical journal 1972; 12:1630-1641.

30. Rabinowitz YS. Keratoconus. Survey of ophthalmology 1998; 42:297-319.

31. Nash IS, Greene PR, Foster CS. Comparison of mechanical properties of keratoconus and normal corneas. Experimental eye research 1982; 35:413-424.

32. Andreassen TT, Hjorth Simonsen A, Oxlund H. Biomechanical properties of keratoconus and normal corneas. Experimental eye research 1980; 31:435-441.

33. Edmund C. Corneal elasticity and ocular rigidity in normal and keratoconic eyes. Acta ophthalmologica 1988; 66:134-140.

34. Wollensak G. Corneal collagen crosslinking: new horizons. Expert Review of Ophthalmology 2010; 5:201-215.

35. Wollensak G. Crosslinking treatment of progressive keratoconus: new hope. Current opinion in ophthalmology 2006; 17:356-360.

36. Wollensak G, Spoerl E, Seiler T. Riboflavin/ultraviolet-A–induced collagen crosslinking for the treatment of keratoconus. American journal of ophthalmology 2003; 135:620-627.

37. Raiskup-Wolf F, Hoyer A, Spoerl E, Pillunat LE. Collagen crosslinking with riboflavin and ultraviolet-A light in keratoconus: long-term results. Journal of Cataract & Refractive Surgery 2008; 34:796-801.

38. Hayes S, Kamma-Lorger CS, Boote C, et al. The effect of riboflavin/UVA collagen cross-linking therapy on the structure and hydrodynamic behaviour of the ungulate and rabbit corneal stroma. PloS one 2013; 8:e52860.

39. Bottos KM, Dreyfuss JL, Regatieri C, et al. Immunofluorescence confocal microscopy of porcine corneas following collagen cross-linking treatment with riboflavin and ultraviolet A. Journal of refractive surgery (Thorofare, NJ: 1995) 2008; 24:S715.

40. Bottós KM, Hofling-Lima AL, Barbosa MC, et al. Effect of collagen cross-linking in stromal fibril organization in edematous human corneas. Cornea 2010; 29:789-793.

41. Wollensak G, Spoerl E, Seiler T. Stress-strain measurements of human and porcine corneas after riboflavin–ultraviolet-A-induced cross-linking. Journal of Cataract & Refractive Surgery 2003; 29:1780-1785.

42. Søndergaard AP, Ivarsen A, Hjortdal J. Corneal resistance to shear force after UVA-riboflavin cross-linking. Investigative ophthalmology & visual science 2013; 54:5059-5069.

43. Søndergaard AP, Ivarsen A, Hjortdal J. Reduction of stromal swelling pressure after UVA-riboflavin cross-linking. Investigative ophthalmology & visual science 2013; 54:1625-1634.

44. Kontadakis GA, Ginis H, Karyotakis N, et al. In vitro effect of corneal collagen cross-linking on corneal hydration properties and stiffness. Graefe's Archive for Clinical and Experimental Ophthalmology 2013; 251:543-547.

45. McCall AS, Kraft S, Edelhauser HF, et al. Mechanisms of corneal tissue cross-linking in response to treatment with topical riboflavin and long-wavelength ultraviolet radiation (UVA). Investigative ophthalmology & visual science 2010; 51:129-138.

46. Spoerl E, Huhle M, Seiler T. Induction of cross-links in corneal tissue. Experimental eye research 1998; 66:97-103.

47. Wollensak G, Iomdina E. Long-term biomechanical properties of rabbit cornea after photodynamic collagen crosslinking. Acta ophthalmologica 2009; 87:48-51.

48. Elsheikh A, Kassem W, Jones SW. Strain-rate sensitivity of porcine and ovine corneas. Acta Bioeng Biomech 2011; 13:25-36.

49. Hoeltzel DA, Altman P, Buzard K, Choe K. Strip extensiometry for comparison of the mechanical response of bovine, rabbit, and human corneas. Journal of Biomechanical Engineering 1992; 114:202.

50. Woo S-Y, Kobayashi A, Schlegel W, Lawrence C. Nonlinear material properties of intact cornea and sclera. Experimental eye research 1972; 14:29-39.

51. Lari DR, Schultz DS, Wang AS, Lee O-T, Stewart JM. Scleral mechanics: comparing whole globe inflation and uniaxial testing. Experimental Eye Research 2012; 94:128-135.

52. Fung Y. Biomechanics: mechanical properties of living tissues. 1993. Springer-Verlag, New York.

53. Fung Y-C. Stress-strain-history relations of soft tissues in simple elongation. Biomechanics: its foundations and objectives 1972; 7:181-208.

54. Kenedi R, Gibson T, Daly C. Structure and function of connective and skeletal tissue. St Andrews, Scotland 1964; 388-395.

55. Decraemer W, Maes M, Vanhuyse V. An elastic stress-strain relation for soft biological tissues based on a structural model. Journal of biomechanics 1980; 13:463-468.

56. Lynch HA, Johannessen W, Wu JP, Jawa A, Elliott DM. Effect of fiber orientation and strain rate on the nonlinear uniaxial tensile material properties of tendon. Journal of biomechanical engineering 2003; 125:726.

57. Provenzano P, Lakes R, Keenan T, Vanderby Jr R. Nonlinear ligament viscoelasticity. Annals of biomedical engineering 2001; 29:908-914.

58. Hubbard RP, Chun KJ. Mechanical responses of tendons to repeated extensions and wait periods. Journal of biomechanical engineering 1988; 110:11-19.

59. Bryant MR, McDonnell PJ. Constitutive laws for biomechanical modeling of refractive surgery. Journal of biomechanical engineering 1996; 118:473.

60. Moon DK, Woo SL, Takakura Y, Gabriel MT, Abramowitch SD. The effects of refreezing on the viscoelastic and tensile properties of ligaments. Journal of biomechanics 2006; 39:1153-1157.

61. Hatami-Marbini H, Etebu E, Rahimi A. Swelling pressure and hydration behavior of porcine corneal stroma. Current eye research 2013; 38:1124-1132.

62. Wright T, Hayes W. Tensile testing of bone over a wide range of strain rates: effects of strain rate, microstructure and density. Medical and biological engineering 1976; 14:671-680.

63. Arumugam V, Naresh M, Sanjeevi R. Effect of strain rate on the fracture behaviour of skin. Journal of Biosciences 1994; 19:307-313.

64. Kim W, Argento A, Rozsa FW, Mallett K. Constitutive Behavior of Ocular Tissues Over a Range of Strain Rates. Journal of biomechanical engineering 2012; 134.

65. Jue B, Maurice DM. The mechanical properties of the rabbit and human cornea. Journal of biomechanics 1986; 19:847-853.

66. Elsheikh A, Alhasso D. Mechanical anisotropy of porcine cornea and correlation with stromal microstructure. Experimental eye research 2009; 88:1084-1091.

67. Hatami-Marbini H, Rahimi A. The relation between hydration and mechanical behavior of bovine cornea in tension. Journal of the mechanical behavior of biomedical materials 2014; 36:90-97.

68. Chimich D, Shrive N, Frank C, Marchuk L, Bray R. Water content alters viscoelastic behaviour of the normal adolescent rabbit medial collateral ligament. Journal of biomechanics 1992; 25:831-837.

69. Haut TL, Haut RC. The state of tissue hydration determines the strain-rate-sensitive stiffness of human patellar tendon. Journal of biomechanics 1997; 30:79-81.

70. Panagiotacopulos N, Bloch R, Knauss W, Harvey P, Patzakis M. On the Mechanical Properties of the Human Intervertebral Disc. DTIC Document; 1978.

71. Atkinson TS, Ewers BJ, Haut RC. The tensile and stress relaxation responses of human patellar tendon varies with specimen cross-sectional area. Journal of biomechanics 1999; 32:907-914.

72. Screen HR, Shelton JC, Chhaya VH, Kayser MV, Bader DL, Lee DA. The influence of noncollagenous matrix components on the micromechanical environment of tendon fascicles. Annals of Biomedical Engineering 2005; 33:1090-1099.

73. Hatami-Marbini H, Etebu E. An experimental and theoretical analysis of unconfined compression of corneal stroma. Journal of biomechanics 2013; 46:1752-1758.

74. Castoro J, Bettelheim A, Bettelheim F. Water gradients across bovine cornea. Investigative ophthalmology & visual science 1988; 29:963-968.

75. Hjortdal JØ. Biomechanical studies of the human cornea. Acta ophthalmologica Scandinavica 1995; 73:364-365.

76. Meek K, Fullwood N, Cooke P, et al. Synchrotron x-ray diffraction studies of the cornea, with implications for stromal hydration. Biophysical journal 1991; 60:467-474.

77. Meek K, Leonard D, Connon C, Dennis S, Khan S. Transparency, swelling and scarring in the corneal stroma. Eye 2003; 17:927-936.

78. Spoerl E, Wollensak G, Seiler T. Increased resistance of crosslinked cornea against enzymatic digestion. Current eye research 2004; 29:35-40.

79. Spoerl E, Mrochen M, Sliney D, Trokel S, Seiler T. Safety of UVA-riboflavin cross-linking of the cornea. Cornea 2007; 26:385-389.

80. Wollensak G, Wilsch M, Spoerl E, Seiler T. Collagen fiber diameter in the rabbit cornea after collagen crosslinking by riboflavin/UVA. Cornea 2004; 23:503-507.

81. Wollensak G, Aurich H, Pham D-T, Wirbelauer C. Hydration behavior of porcine cornea crosslinked with riboflavin and ultraviolet A. Journal of Cataract & Refractive Surgery 2007; 33:516-521.

82. Kohlhaas M, Spoerl E, Schilde T, Unger G, Wittig C, Pillunat LE. Biomechanical evidence of the distribution of cross-links in corneastreated with riboflavin and ultraviolet A light. Journal of Cataract & Refractive Surgery 2006; 32:279-283.

83. Coskunseven E, Jankov M, Hafezi F. Comparative study of corneal collagen cross-linking with riboflavin and UVA irradiation in patients with keratoconus. J Refract Surg 2009; 25:371-376.

84. Wollensak G, Spoerl E, Wilsch M, Seiler T. Keratocyte apoptosis after corneal collagen cross-linking using riboflavin/UVA treatment. Cornea 2004; 23:43-49.

85. Hatami-Marbini H, Rahimi A. Effects of bathing solution on tensile properties of the cornea. Experimental eye research 2013.

86. Zhang Y, Conrad AH, Conrad GW. Effects of ultraviolet-A and riboflavin on the interaction of collagen and proteoglycans during corneal cross-linking. Journal of Biological Chemistry 2011; 286:13011-13022.

87. Puxkandl R, Zizak I, Paris O, et al. Viscoelastic properties of collagen: synchrotron radiation investigations and structural model. Philosophical Transactions of the Royal Society of London Series B: Biological Sciences 2002; 357:191-197.

88. Müller LJ, Pels E, Schurmans LR, Vrensen GF. A new three-dimensional model of the organization of proteoglycans and collagen fibrils in the human corneal stroma. Experimental eye research 2004; 78:493-501.

89. Hjortdal JØ. Extensibility of the normo-hydrated human cornea. Acta Ophthalmologica Scandinavica 1995; 73:12-17.

90. Weeber HA, Eckert G, Soergel F, Meyer CH, Pechhold W, van der Heijde RG. Dynamic mechanical properties of human lenses. Experimental eye research 2005; 80:425-434.

91. Bettelheim FA, Wang TJ. Dynamic viscoelastic properties of bovine vitreous. Experimental eye research 1976; 23:435-441.

92. Kaufmann C, Bachmann LM, Robert YC, Thiel MA. Ocular pulse amplitude in healthy subjects as measured by dynamic contour tonometry. Archives of ophthalmology 2006; 124:1104-1108.

93. Palko JR, Pan X, Liu J. Dynamic testing of regional viscoelastic behavior of canine sclera. Experimental eye research 2011; 93:825-832.

94. Liu Z, Bilston L. On the viscoelastic character of liver tissue: experiments and modelling of the linear behaviour. Biorheology 2000; 37:191-201.

95. Netti P, D'amore A, Ronca D, Ambrosio L, Nicolais L. Structure-mechanical properties relationship of natural tendons and ligaments. Journal of Materials Science: Materials in Medicine 1996; 7:525-530.

96. Tanaka E, Inubushi T, Takahashi K, et al. Dynamic shear properties of the porcine molar periodontal ligament. Journal of biomechanics 2007; 40:1477-1483.

97. Palko JR, Iwabe S, Pan X, Agarwal G, Komáromy AM, Liu J. Biomechanical Properties and Correlation With Collagen Solubility Profile in the Posterior Sclera of Canine Eyes With an ADAMTS10 Mutation. Investigative ophthalmology & visual science 2013; 54:2685-2695.

98. Schechtman H, Bader D. Dynamic characterization of human tendons. Proceedings of the Institution of Mechanical Engineers, Part H: Journal of Engineering in Medicine 1994; 208:241-248.

99. Mijailovich SM, Stamenovic D, Brown R, Leith DE, Fredberg JJ. Dynamic moduli of rabbit lung tissue and pigeon ligamentum propatagiale undergoing uniaxial cyclic loading. Journal of Applied Physiology 1994; 76:773-782.

100. Silver FH, Freeman JW, DeVore D. Viscoelastic properties of human skin and processed dermis. Skin Research and Technology 2001; 7:18-23.

101. Silver FH, Horvath I, Foran DJ. Viscoelasticity of the vessel wall: the role of collagen and elastic fibers. Critical Reviews™ in Biomedical Engineering 2001; 29.

102. Kesava Reddy G. AGE-related cross-linking of collagen is associated with aortic wall matrix stiffness in the pathogenesis of drug-induced diabetes in rats. Microvascular Research 2004; 68:132-142.

103. Reddy GK. Cross-linking in collagen by nonenzymatic glycation increases the matrix stiffness in rabbit achilles tendon. Experimental Diabetes Research 2004; 5:143-153.

104. Eisenberg SR, Grodzinsky AJ. The kinetics of chemically induced nonequilibrium swelling of articular cartilage and corneal stroma. Journal of biomechanical engineering 1987; 109:79-89.

105. Pandolfi A, Manganiello F. A model for the human cornea: constitutive formulation and numerical analysis. Biomechanics and modeling in mechanobiology 2006; 5:237-246.

VITA

Abdolrasol Rahimi

Candidate for the Degree of

Master of Science

Thesis: CHARACTERIZATION OF BIOMECHANICAL PROPERTIES OF THE BOVINE CORNEA IN TENSION

Major Field: Mechanical and Aerospace Engineering

Biographical:

Education:

Completed the requirements for the Master of Science/Arts in your major at Oklahoma State University, Stillwater, Oklahoma in July, 2014.

Completed the requirements for the Bachelor of Science/Arts in your major at Amirkabir University, Tehran, Iran in June 2011.

Experience:

Research Assistant January 2012-Present
Computational Biomechanics Lab, Oklahoma State University, Stillwater, OK

- Designed and built a tensile testing device which was used for experiments on connective tissues
- Developed testing protocols used to performed static and dynamic mechanical tests
- Analyzed the stress relaxation and strain rate dependent behavior of soft tissues

Teaching Assistant January 2012-Present
For Measurement and Instrumentation, Mechanical Design, and Dynamics course
Mechanical Engineering Department, Oklahoma State University, Stillwater, OK

- Accomplished exam and homework grading
- Assisted students to get a better understanding of theories in discussion sessions